iScience

CellPress
OPEN ACCESS

Article

# Plant Toll/interleukin-1 receptor/resistance protein domains physically associate with enhanced disease susceptibility1 family proteins in immune signaling

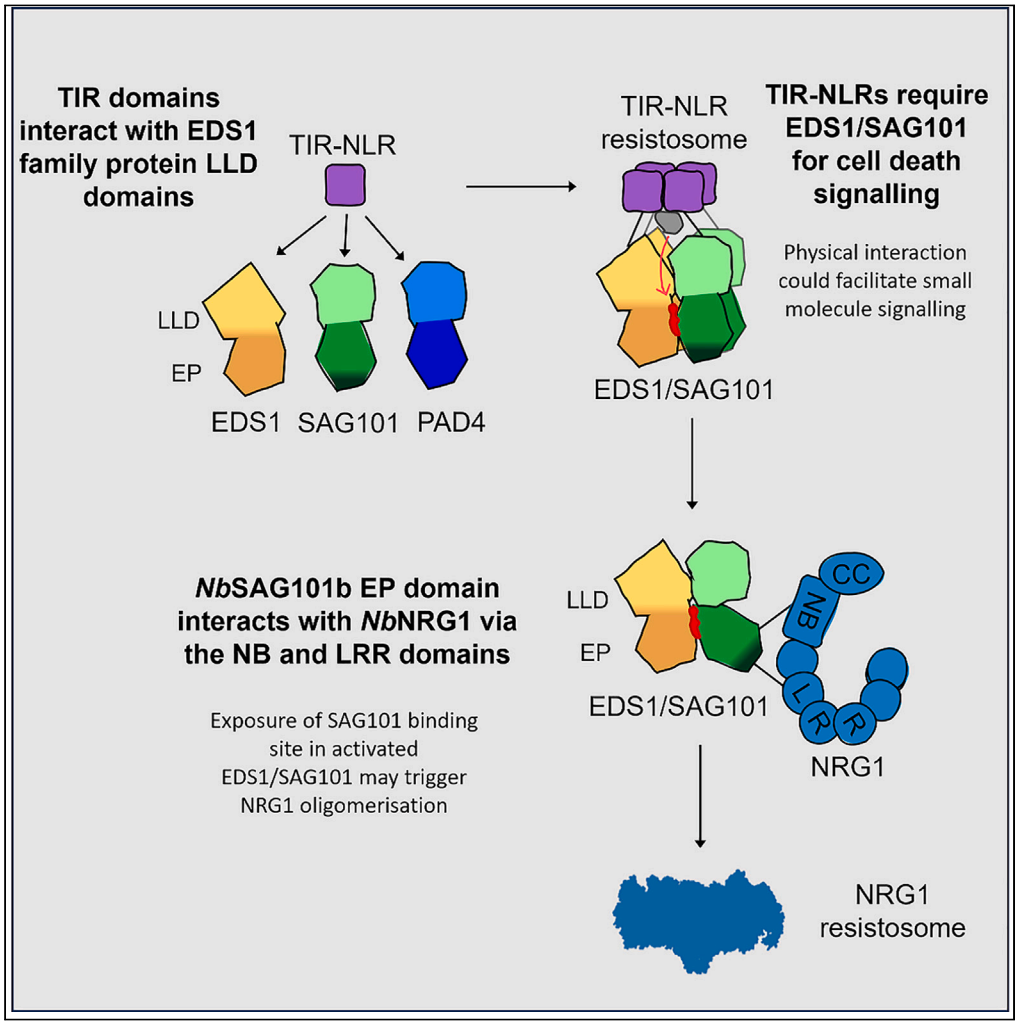


Jian Chen, Xiaoxiao Zhang, Maud Bernoux, John P. Rathjen, Peter N. Dodds

peter.dodds@csiro.au

## Highlights

Diverse TIR-NLRs require *Nb*EDS1-*Nb*SAG101b-*Nb*NRG1 for cell death signaling

TIR domains associate with *Nb*EDS1, *Nb*PAD4, and *Nb*SAG101 *in planta*

*Nb*NRG1 specifically interacts with *Nb*SAG101b via its C-terminal EP domain

Chen et al., iScience *27*, 108817
February 16, 2024 
https://doi.org/10.1016/j.isci.2024.108817

iScience

CellPress
OPEN ACCESS

Article

# Plant Toll/interleukin-1 receptor/resistance protein domains physically associate with enhanced disease susceptibility1 family proteins in immune signaling

Jian Chen,[1,2] Xiaoxiao Zhang,[2] Maud Bernoux,[3] John P. Rathjen,[2] and Peter N. Dodds[1,4,*]

## SUMMARY

**Plant Toll/interleukin-1 receptor/resistance protein (TIR) type nucleotide-binding and leucine-rich repeat immune receptors (NLRs) require enhanced disease susceptibility 1 (EDS1) family proteins and the helper NLRs NRG1 and ADR1 for immune activation. We show that the *Nb*EDS1-*Nb*SAG101b-*Nb*NRG1 signaling pathway in *N. benthamiana* is necessary for cell death signaling by TIR-NLRs from a range of plant species, suggesting a universal requirement for this module in TIR-NLR-mediated cell death in *N. benthamiana*. We also find that TIR domains physically associate with *Nb*EDS1, *Nb*PAD4, and *Nb*SAG101 *in planta*, independently of each other. Furthermore, *Nb*NRG1 associates with *Nb*SAG101b, but not with other EDS1 family members, via its C-terminal EP domain. Physical interaction between activated TIRs and EDS1 signaling complexes may facilitate the transfer of low abundance products of TIR catalytic activity or alter TIR catalytic activity to favor the production of EDS1 heterodimer ligands.**

## INTRODUCTION

The plant immune system consists of two main layers of pathogen perception.[1–3] Membrane-bound pattern recognition receptors (PRRs) monitor the extracellular space and can detect pathogen-derived molecules in the apoplast to trigger pattern-triggered immunity (PTI). Intracellular receptors recognize pathogen effectors that are delivered into the plant cell and activate effector-triggered immunity (ETI), which is often associated with a hypersensitive response (HR) involving localized cell death. Most intracellular resistance proteins belong to the nucleotide-binding domain leucine-rich repeat (NLR) class, with either an N-terminal TIR (Toll/interleukin-1 receptor/resistance protein) or CC (coiled-coil) signaling domain.[4–6] Cryo-EM structural analysis of the *Arabidopsis* resistance protein ZAR1 showed that the CC signaling domain adopts a four-helix bundle fold in the inactive monomer state, while effector recognition leads to the formation of a pentamer in which the previously buried α1 helix of the CC domain protrudes to form the point of the funnel.[7,8] This activated ZAR1 resistosome complex localizes to the plasma membrane and has calcium-permeable cation-selective channel activity that is required for cell death signaling.[9] The wheat Sr35 CC-NLR resistosome revealed a similar pentameric structure and calcium channel activity,[10] suggesting conserved activation and signaling patterns across CC-NLRs. TIR domains require self-association for cell death signaling activity[11–13] and exhibit an NADase catalytic activity which can cleave $NAD^+$ to produce nicotinamide and a variant cyclic-ADPR (v-cADPR) *in vitro*.[14,15] TIR signaling can be activated by forced oligomerisation through fusion to the tandem SAM domains of the human SARM1 protein, which form an octameric ring assembly,[15] or to the mammalian NLRC4 immune receptor which forms an oligomeric inflammasome in cooperation with NAIP NLRs and a corresponding ligand,[16–18] or to the flax rust effector AvrM, which forms a stable dimer *in planta*.[19] Activated full-length TIR-NLRs RPP1 and Roq1 form tetramers where the TIR domains self-associate resulting in conformational changes that expose the NADase catalytic sites in two of the four TIR subunits,[20,21] providing an explanation for how effector-driven TIR-NLR oligomerization leads to signaling activation via its catalytic function.

TIR-NLR signaling requires two layers of downstream partners. The first layer includes the EDS1 (enhanced disease susceptibility 1) family lipase-like proteins. EDS1 forms distinct heterodimers with the related protein family members PAD4 (phytoalexin deficient 4) or SAG101 (senescence-associated gene 101).[22–25] The second layer includes two families of helper NLRs of the RPW8-like CC-NLR class, NRG1 and ADR1. These work cooperatively with either the EDS1-SAG101 or EDS1-PAD4 heterocomplexes respectively, to mediate immunity.[26–31] EDS1, PAD4, and SAG101 share similar structures with N-terminal lipase-like domains (LLD) and C-terminal EDS1-PAD4 domains (EP).[23,25,32] The heterodimer interaction is mainly mediated through a convex-concave interface formed by the protruding hydrophobic α-H helix of the EDS1 LLD domain that fits into a hydrophobic pocket of the LLD domains of SAG101 or PAD4.[25,33,34] Mutations of

[1]Commonwealth Scientific and Industrial Research Organization, Agriculture and Food, Canberra, ACT 2601, Australia
[2]Research School of Biology, The Australian National University, Canberra, ACT 2600, Australia
[3]Laboratoire des interactions plantes-microbes-environnement, Université de Toulouse, INRAE, CNRS, Castanet-Tolosan, France
[4]Lead contact
*Correspondence: peter.dodds@csiro.au
https://doi.org/10.1016/j.isci.2024.108817

hydrophobic residues in the EDS1 α-H helix or in the SAG101 or PAD4 hydrophobic pockets greatly weaken the heterodimer interactions and also abrogate the signaling functions of Arabidopsis and tomato EDS1-family proteins.[25,34] Characterization of Arabidopsis EDS1 heterodimers purified from insect cells after RPP1 activation detected 2'-(5"-phosphoribosyl)-5'-adenosine mono- or di-phosphate (pRib-AMP/ADP) and ADP-ribosylated ATP or ADP-ribosylated ADP ribose (ADPr-ATP/di-ADPR) specifically bound to pockets formed by the EP domains of EDS1-PAD4 and EDS1-SAG101 heterodimers respectively.[35,36] These TIR-catalysed small molecules allosterically promote interaction between EDS1 heterodimers and their respective NRG1 or ADR1 helper proteins. Similar to ZAR1 and Sr35, activated NRG1 and ADR1 oligomerise, associate with membranes and form calcium-permeable cation channels necessary to trigger immunity and cell death.[37,38] The discrepancies between the *in vitro* activities of isolated TIRs and the signaling molecules associated with EDS1 heterodimers are not understood.[39] Here we have examined protein-protein interactions in the TIR-EDS family pathway to shed further light on the signal transduction process.

In *N. benthamiana*, induction of cell death by the autoactive isolated *At*RPS4TIR and *At*DM2hTIR domains or by the effector activation of the intact N and Roq1 TIR-NLRs requires *Nb*SAG101b but not *Nb*SAG101a or *Nb*PAD4.[27,31,34] *Nb*NRG1 is also required for cell death mediated by Roq1, N, *At*RPP1, and *At*DM2h in *N. benthamiana*.[40] Here we show that the *Nb*EDS1-*Nb*SAG101b-*Nb*NRG1 signaling module in *N. benthamiana* is necessary and sufficient for cell death signaling by six additional TIR-containing NLRs from a range of plant species, suggesting it is likely a universal requirement for TIR-NLR-mediated cell death in this species. We also find that TIR domains can physically interact with *Nb*EDS1, *Nb*PAD4 and *Nb*SAG101 via their LLD domains, while *Nb*NRG1 specifically associates with *Nb*SAG101b via its EP domain, but this is inhibited by *Nb*EDS1/*Nb*SAG101b interaction. These data suggest that the TIR NADase-derived signal may be directly transferred to the EDS1 heterocomplex signaling modules to activate downstream signaling via exposure to a helper NLR binding surface.

## RESULTS

### *Nb*EDS1, *Nb*SAG101b, and *Nb*NRG1 are required for cell death mediated by diverse Toll/interleukin-1 receptor/resistance protein-nucleotide-binding and leucine-rich repeat immune receptors in *N. benthamiana*

We tested the ability of the TIR domains of six TIR-NLRs from flax (L6, M and M1), grapevine (Run1) and Arabidopsis (SNC1 and RPS4) to induce cell death in the *N. benthamiana* single, double, or triple gene knockout lines *eds1*, *eds1/pad4*, *pad4/sag101a/sag101b* (denoted *pss*) and *nrg1*. The TIR domains were tested in different contexts that induce cell death (Figure S1), including: autoactive TIR-alone fragments; full-length TIR-NLRs co-expressed with corresponding Avr proteins; full-length autoactive mutant TIR-NLRs; and TIR domain fusions to either the oligomerising SAM domain of SARM1[15] or to the animal receptor NLRC4 co-expressed with NAIP5 and ligand FlaA.[16] Individual expression of all 16 constructs induced visible cell death in wildtype (WT) *N. benthamiana* leaves, but none caused detectable cell death in *eds1* plants (Figures 1A and S2) except for those containing the RPS4 TIR domain, which induced very weak cell death. The cell death induced by the expression of each of these 16 constructs in *eds1* plants was restored to the level of WT leaves by the co-expression of *Nb*EDS1. The residual cell death observed for the RPS4TIR series in *eds1* plants was abolished when the NADase catalytic site glutamate was mutated to alanine (E88A) and in the case of SAM-RPS4TIR-3Myc when the wildtype SAM domain was replaced with the non-oligomerizing SAM5M fusion (Figure S3). Thus, RPS4TIR residual cell death was dependent on both oligomerization and NADase activity.

TIR-mediated cell death was also abolished in *eds1/pad4* double knockout plants and could be recovered with the co-expression of *Nb*EDS1 but not *Nb*PAD4 (Figures 1B and S4). Co-expression with both *Nb*PAD4 and *Nb*EDS1 complemented cell death to similar levels as *Nb*EDS1 alone. Similarly, TIR-induced cell death was abolished in leaves of the *pss* triple gene knockout and could be recovered by the co-expression of *Nb*SAG101b, but not *Nb*PAD4 or *Nb*SAG101a alone or in combination (Figures 1C and S5). Co-expression of *Nb*PAD4 and *Nb*SAG101a with *Nb*SAG101b did not affect the complementation of cell death. None of the TIR-containing constructs induced cell death in *nrg1* leaves, but this phenotype was recovered by co-expression with *Nb*NRG1, although not fully to the wild-type levels (Figures 1D and S6A). The RPS4TIR series also retained a weak cell death activity in *eds1/pad4*, *pss*, and *nrg1* plants, possibly indicating a limited capacity of the RPS4 TIR to induce a weak cell death response by another unknown pathway. Overall, these data extend the observation that TIR-NLR-mediated cell death in *N. benthamiana* generally requires *Nb*EDS1, *Nb*SAG101b, and *Nb*NRG1, but not *Nb*PAD4 or *Nb*SAG101a, as reported previously for a few TIR-NLRs.[31,34]

Although NRG1 overexpression was previously reported to cause cell death in *N. benthamiana*,[27,30,41] we did not observe this with *Nb*NRG1-3xHA or *Nb*NRG1-YFP expression in the above experiments using the pAM-PAT-35S vector. However, expression of *Nb*NRG1-3xHA from the pBIN19-35S vector caused a strong cell death phenotype (Figure S7). Similarly, *Nb*ADR1-3xHA fusions showed strong cell death when expressed from pBIN19-35S but not from pAM-PAT-35S. In both cases, this correlated with a higher accumulation of protein after expression from the pBIN19-35S vector. This is consistent with the results of Qi et al.,[27] who found that the lower expression of *Nb*NRG1 from its native promoter could complement TIR-NLR induced cell death in the *nrg1* mutant plants without autoactive cell death. The pAM-PAT-35S-driven *Nb*NRG1 only partially complemented TIR-mediated cell death in *nrg1* plants, but surprisingly also partially inhibited cell death in WT plants (Figure S6B), suggesting that moderately high expression may interfere with normal TIR-EDS1/SAG101-mediated cell death. The higher expressing pBIN19-*Nb*NRG1 and pBIN19-*Nb*ADR1 constructs also induced strong cell death in the *eds1*, *eds1pad4*, *pss*, and *nrg1* mutant plants (Figure S7), consistent with the role of these helper NLRs downstream of EDS1 family proteins in *N. benthamiana*. Co-expression of the wheat CC-NLR protein Sr50 with AvrSr50, or expression of the autoactive CC domains of Sr50 or *Nb*NRG1 caused strong cell death

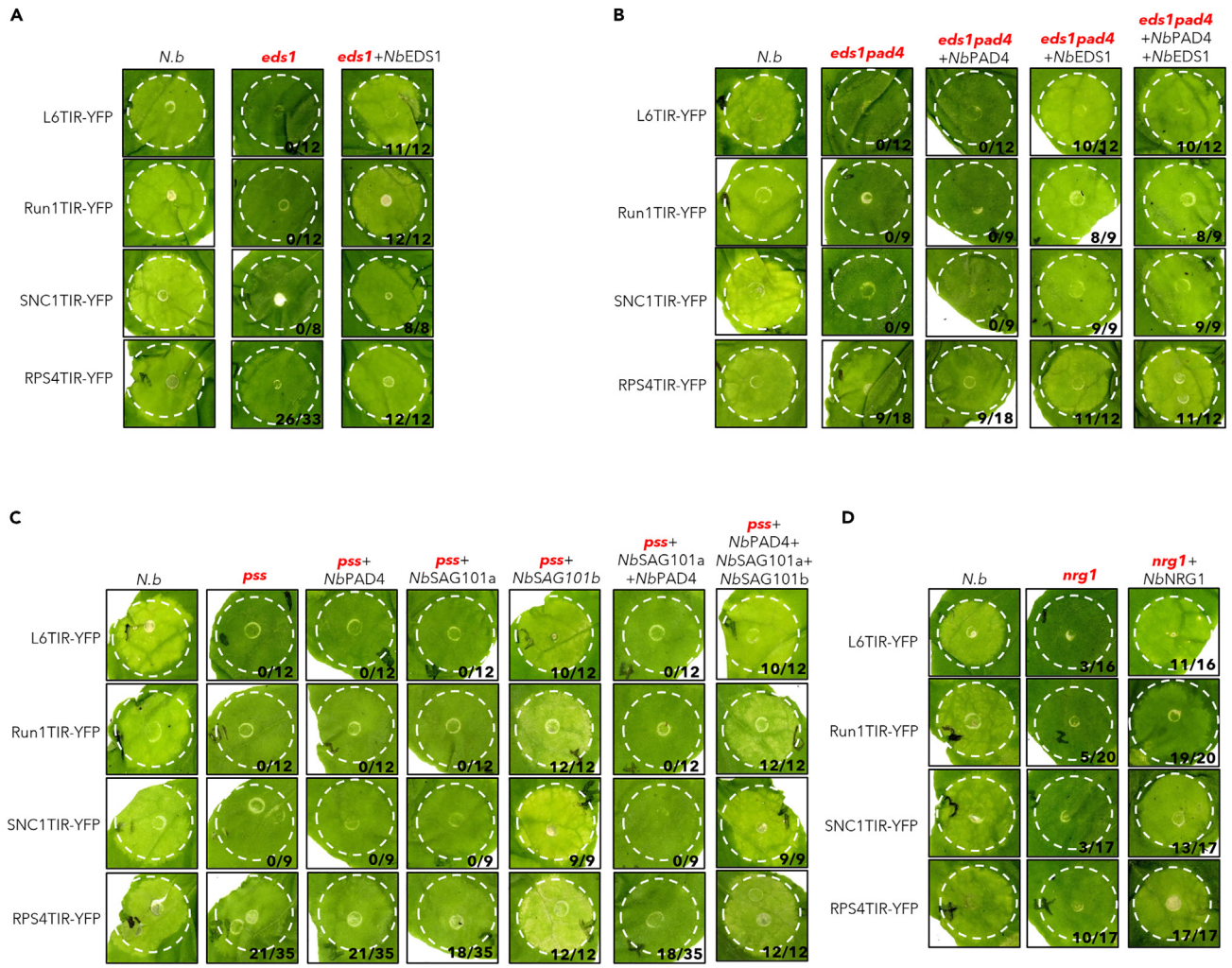


**Figure 1. *Nb*EDS1, *Nb*SAG101b, and *Nb*NRG1 are required for TIR mediated cell death in *N. benthamiana***

(A–D) Complementation of TIR-mediated cell death in the *eds1* (A), *eds1pad4* (B), *pad4sag101a/sag101b* (*pss*) (C), and *nrg1* (D) mutant lines of *N. benthamiana*. The indicated TIR proteins fused to YFP were expressed alone in wild-type (*N.b.*) or mutant lines or in combination with *Nb*EDS1 family proteins or NRG1 fused to 3xHA in the mutant lines by Agrobacterium-mediated transient expression with the bacterial concentration at OD600 = 0.5. Photos were taken at 5 days post infiltration (dpi). This experiment was repeated at least 5 times. Numbers on each image indicates the number of infiltrations show complemented cell death out of the total number of infiltrations performed.

in WT and all mutant *N. benthamiana* lines, further validating that EDS1, SAG101, and NRG1 are required for TIR but not CC-mediated signaling (Figure S8).

## TIR domains associate with *Nb*EDS1, *Nb*PAD4, and *Nb*SAG101b in co-immunoprecipitation assays

To test whether signal transduction from TIR-NLRs to the EDS1 module might involve the physical association of the proteins, we co-expressed TIR domain and EDS1 family proteins with either YFP or 3xHA tags and pulled down the YFP-labelled protein with anti-GFP beads to test for co-immunoprecipitation (Co-IP). All four tested autoactive plant TIR-3xHA fusions co-precipitated with *Nb*EDS1-YFP, and conversely, *Nb*EDS1-3xHA could be co-precipitated with each of the TIR-YFP fusions (Figure 2A). In contrast, neither YFP alone nor the CC domain of Sr50 (Sr50CC-3HA) showed association with *Nb*EDS1 (fused to 3xHA or YFP) (Figures 2A and 2B), and neither 3xHA nor YFP-tagged TIRs co-immunoprecipitated with YFP alone or the Sr50CC-3xHA respectively (Figure S9A). These TIR-*Nb*EDS1 associations were also observed in *pss* plants (Figures 2B and S9B), indicating they were independent of *Nb*PAD4, *Nb*SAG101a, and *Nb*SAG101b. Co-expression of a Myc-tagged *Nb*SAG101b protein did not affect the association between these TIR domains and *Nb*EDS1 (Figure S9C).

Mutation of the key NADase catalytic site glutamate to alanine (E to A) in the four TIR domains consistently resulted in enhanced pull-down of *Nb*EDS1 compared to the wildtype TIRs (Figure 2B) and was most apparent for Run1TIR (Figure S9D). On the other hand, the Run1TIR RRAA (R64A + R65A) mutant, which has enhanced NADase activity,[15] showed similar association with *Nb*EDS1 compared with Run1TIR. Mutations

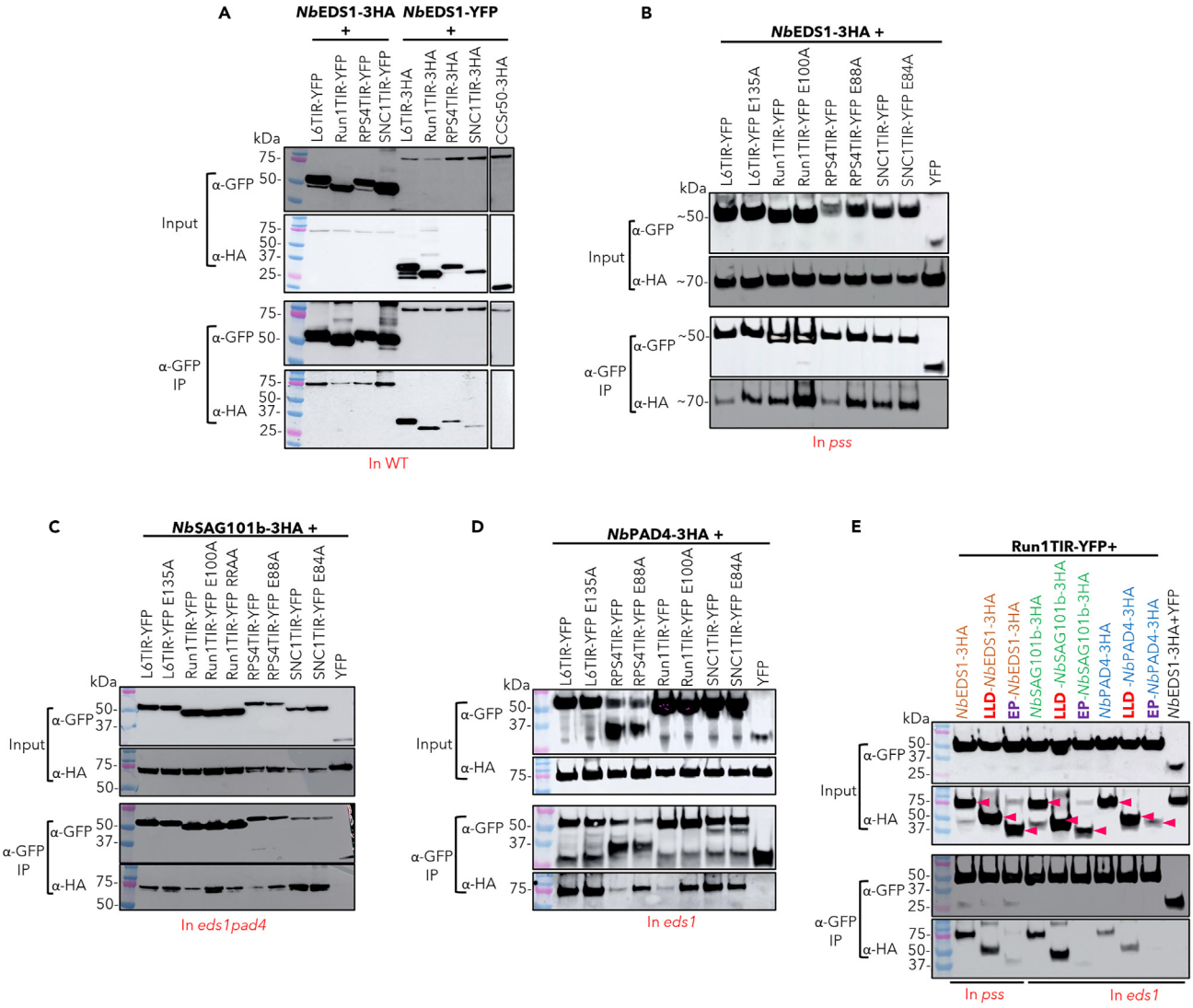


**Figure 2. Plant TIRs interact with EDS1 family proteins in co-immunoprecipitation experiments *in planta***

*Nb*EDS1, *Nb*SAG10, *Nb*PAD4, and TIR proteins fused to YFP or 3xHA tags were transiently co-expressed in wildtype or mutant *N. benthamiana* leaves in the indicated combinations and proteins were extracted after 24 h. Tagged proteins were detected in the extract (input) and after immunoprecipitation with anti-GFP beads (IP) by immunoblotting with anti-HA (α-HA) or anti-GFP (α-GFP) antibodies. YFP alone or an Sr50 CC domain YFP fusion (CCSr50-YFP) were included as negative controls as indicated. (A) Reciprocal Co-IP experiments between TIR-YFP protein fusions with *Nb*EDS1-3xHA and *Nb*EDS1-YFP with TIR-3xHA expressed in wildtype plants (B). Co-IP experiments of *Nb*EDS1-3xHA with TIR-YFP and NADase catalytic site mutants (E135A and so forth) expressed in *pad4/sag101a/sag101b* plants.

(C) Co-IP experiments of *Nb*SAG101b-3xHA with wildtype and catalytic mutant TIR-YFP fusions expressed in *eds1pad4* plants.

(D) Co-IP experiments of *Nb*PAD4-3xHA with wildtype and catalytic mutant TIR-YFP fusions expressed transiently in *eds1* mutant plants.

(E) Co-IP experiments of truncated *Nb*EDS1, *Nb*PAD4 and *Nb*SAG101 proteins fused to a 3xHA tag with Run1TIR-YFP expressed in *pss* (for EDS fusions) or *eds1* (for SAG101 and PAD4) plants. LLD, N-terminal lipase-like domain. EP, C-terminal EP domain.

that disrupted the self-association of L6TIR[11,13] did not affect the ability of L6TIR to pull down *Nb*EDS1 by Co-IP (Figure S9E). These data suggest that TIR-EDS1 association does not require TIR oligomerization or NADase activity.

Both *Nb*PAD4-HA and *Nb*SAG101b-HA co-immunoprecipitated with the TIR-YFP fusion proteins in anti-GFP pull downs in *eds1/pad4* or *eds1* plants (Figures 2C and 2D), indicating that their associations were independent of *Nb*EDS1. Again, RPS4TIR and Run1TIR proteins containing NADase catalytic site mutations also showed stronger association with *Nb*PAD4 and *Nb*SAG101b, although this was not apparent for L6 and SNC1 TIRs. The plant TIRs could also associate with Arabidopsis EDS1, PAD4 and SAG101 (Figure S10), indicating the conservation of this capability between diverse plant species. Co-IP experiments with truncated *Nb*EDS1, *Nb*PAD4 and *Nb*SAG101b

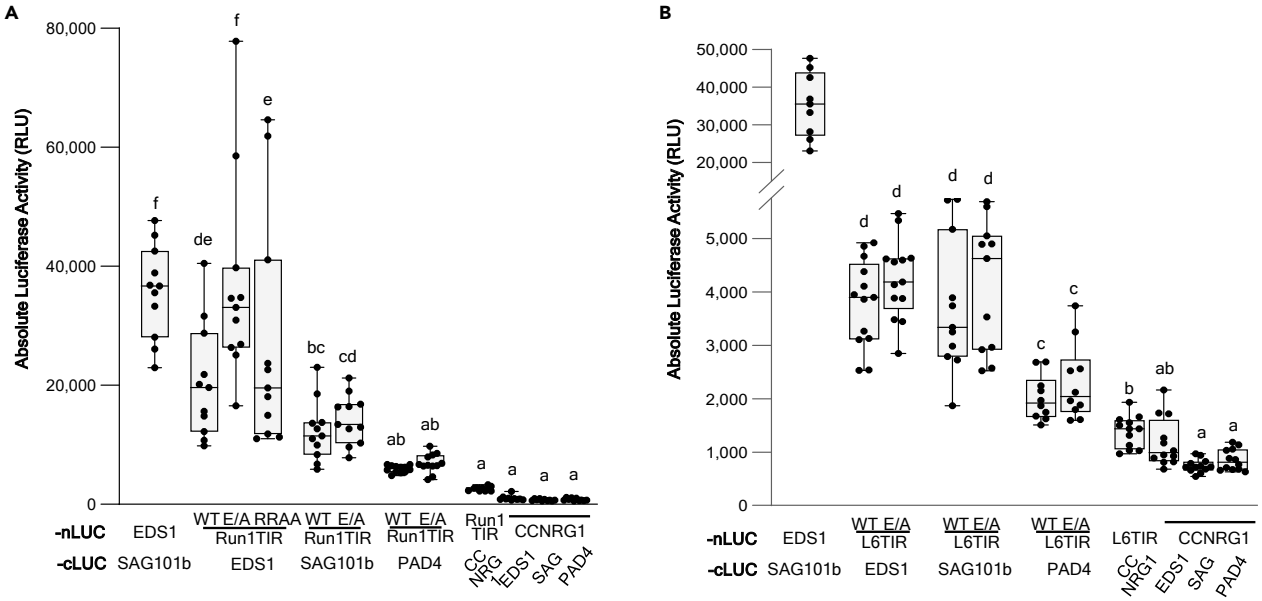
A
Absolute Luciferase Activity (RLU)
80,000
60,000
40,000
20,000
0
f
de
f
e
bc
cd
ab
ab
a
a
a
a
-nLUC EDS1 WT E/A RRAA Run1TIR WT E/A Run1TIR WT E/A Run1TIR Run1 TIR CCNRG1
-cLUC SAG101b EDS1 SAG101b PAD4 CC NRG1 EDS1 SAG PAD4
B
Absolute Luciferase Activity (RLU)
50,000
40,000
30,000
20,000
5,000
4,000
3,000
2,000
1,000
0
d
d
d
d
c
c
b
ab
a
a
-nLUC EDS1 WT E/A L6TIR WT E/A L6TIR WT E/A L6TIR L6TIR CCNRG1
-cLUC SAG101b EDS1 SAG101b PAD4 CC NRG1 EDS1 SAG PAD4

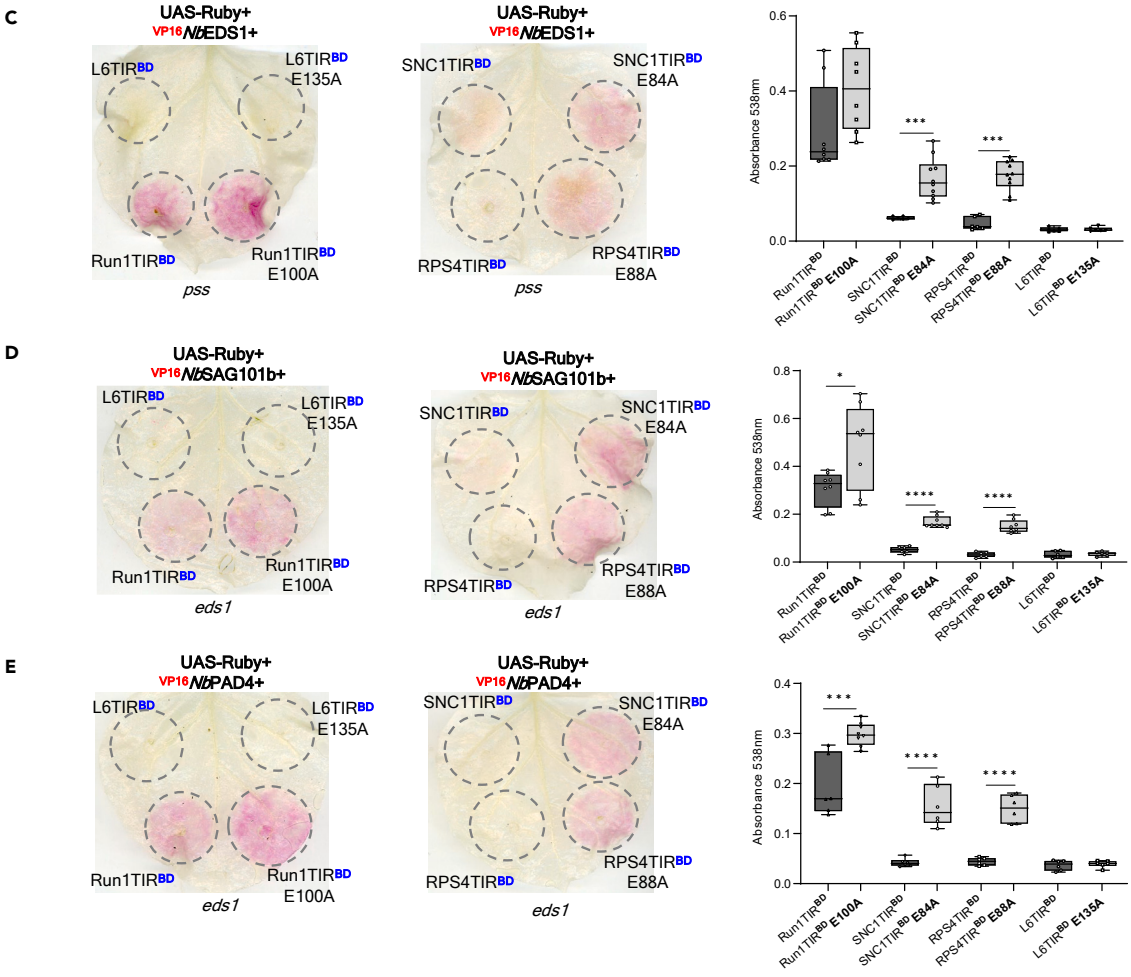
C
UAS-Ruby+
VP16NbEDS1+
L6TIRBD
L6TIRBD E135A
Run1TIRBD
Run1TIRBD E100A
pss
SNC1TIRBD
SNC1TIRBD E84A
RPS4TIRBD
RPS4TIRBD E88A
pss
Absorbance 538nm
0.6
0.4
0.2
0.0
***
***
Run1TIRBD
Run1TIRBD E100A
SNC1TIRBD E84A
SNC1TIRBD E84A
RPS4TIRBD E88A
RPS4TIRBD E88A
L6TIRBD
L6TIRBD E135A
D
UAS-Ruby+
VP16NbSAG101b+
L6TIRBD
L6TIRBD E135A
Run1TIRBD
Run1TIRBD E100A
eds1
SNC1TIRBD
SNC1TIRBD E84A
RPS4TIRBD
RPS4TIRBD E88A
eds1
Absorbance 538nm
0.8
0.6
0.4
0.2
0.0
*
****
****
E
UAS-Ruby+
VP16NbPAD4+
L6TIRBD
L6TIRBD E135A
Run1TIRBD
Run1TIRBD E100A
eds1
SNC1TIRBD
SNC1TIRBD E84A
RPS4TIRBD
RPS4TIRBD E88A
eds1
Absorbance 538nm
0.4
0.3
0.2
0.1
0.0
***
****
****

**Figure 3. Plant TIRs interact with EDS1 family proteins in split luciferase and two-hybrid assays *in planta***

(A) Luciferase activity detected in leaf extracts expressing Run1TIR-nLUC with *Nb*EDS1, *Nb*SAG101b, or *Nb*PAD4 fused to cLUC.

(B) Luciferase activity detected in leaf extracts expressing L6TIR-nLUC with *Nb*EDS1, *Nb*SAG101b, or *Nb*PAD4 fused to cLUC. EDS1-nLUC expressed with SAG101b-cLUC was used as a positive control. Co-expression of a truncated CC domain of *Nb*NRG1 (CC-NRG1) fused to -cLUC or –nLUC with the TIR-nLUC or *Nb*EDS1, SAG101, or PAD4-cLUC fusions served as negative controls. Leaf samples were taken at two dpi. Data are represented as box and whisker plot, with median displayed. The letters on the top of each column indicate statistically differences between different tests (one-way-ANOVA, LSD test, $p < 0.05$). All experiments were conducted in *eds1* plants except the combinations of TIR-nLUC and EDS1-cLUC which were performed in *pss* plants.

(C–E) Plant two-hybrid assays. Betalain accumulation was observed in leaves expressing UAS-Ruby with TIRs fused to BD and *Nb*EDS1, *Nb*SAG101b, *Nb*PAD4 fused to VP16 3–5 days after infiltration. The right box and whisker plots show the absorbance at 538 nm of betalain extracted from the left leaves, with median displayed. Asterisks above columns indicate significant difference between wildtype TIR and the NADase site mutations. *P, 0.05, ***P, 0.001, ****P, 0.0001; Student's t-test.

fragments showed that Run1TIR associated most strongly with the LLD domain of each protein, but only weakly or not at all with the EP domains (Figure 2E).

## TIR domains associate with *Nb*EDS1, *Nb*PAD4, and *Nb*SAG101 in split-luciferase and plant two-hybrid assays

We further confirmed the TIR-EDS1 family protein associations observed in Co-IP experiments by using two independent *in planta* assays. Firstly, for split-luciferase complementation,[42] the N- and C-terminal fragments of the firefly luciferase protein (nLUC and cLUC) were separately fused to L6TIR, Run1TIR, and *Nb*EDS1 family proteins. All fusion proteins retained their normal function when expressed in *N. benthamiana* (autoactivity of TIR domains, Figure S11A; and complementation of signaling mutants by EDS1 family proteins; Figure S11B) and were detected by immunoblotting with anti-luciferase (Figure S11C).

To test for physical association, Run1TIR and L6TIR fused to nLUC were co-expressed with EDS1 family members fused to cLUC in either *eds1* or *pss* plants to eliminate the effects of cell death (Figure 3). Co-expression of nLUC-EDS1 with cLUC-SAG101b resulted in strong luciferase activity as a positive control. Co-expression of Run1TIR-nLUC with *Nb*EDS1-cLUC also resulted in high luciferase activity, while its co-expression with *Nb*SAG101b-cLUC and *Nb*PAD4-cLUC gave lower levels of luciferase activity (Figures 3A and S11D). Similarly, co-expression of L6TIR-nLUC with *Nb*EDS1 family -cLUC fusions showed enhanced luciferase activity compared to the negative controls, (L6TIR-nLUC +-NRG1CC-cLUC, and CCNRG1-nLUC EDS1-cLUC family), with the L6TIR-*Nb*EDS1 and L6TIR-*Nb*SAG101 associations stronger than observed for L6TIR-*Nb*PAD4 (Figure 3B). Although the Run1TIR E100A mutant showed higher luciferase activity than wildtype when paired with *Nb*EDS1-cLUC, this was not seen for Run1TIR E100A paired with *Nb*SAG101 or *Nb*PAD4, or in tests with the equivalent L6TIR E135A mutant. Split-luciferase assays with truncated EDS1 family proteins showed significantly higher activity for the LLD domains fused to cLUC when co-expressed with Run1TIR-nLUC than the equivalent EP domain fused to cLUC (Figures S11C and S11D). Indeed, the LLD domains of *Nb*SAG101b and *Nb*PAD4 showed stronger association with Run1TIR than with the full-length proteins or the EP domain, which is consistent with Co-IP data (Figure 2E).

We also tested associations between TIRs and EDS family proteins using a recently established plant two-hybrid assay based on the yeast GAL4 transcription factor driving the expression of the reporter *Ruby* which produces a purple pigment, betalain, as a readout for protein-protein interaction.[43] These assays were conducted in *eds1* and *pss* plants as above to prevent cell death. Co-expression of Run1TIR or Run1TIR E100A fused to the GAL4 DNA binding domain (Run1TIR$^{BD}$, Run1TIR$^{BD}$ E100A) with *Nb*EDS1 fused to the VP16 activation domain ($^{VP16}$*Nb*EDS1) led to strong betalain accumulation (Figure 3C), confirming a physical association between these proteins. The NADase mutants of SNC1 and RPS4 (SNC1TIR$^{BD}$ E84A or RPS4TIR$^{BD}$ E88A) also showed significant betalain accumulation when co-expressed with $^{VP16}$*Nb*EDS1 indicating physical association, while betalain production was very low for the wildtype SNC1TIR$^{BD}$ or RPS4TIR$^{BD}$ constructs, again indicating a stronger association for the catalytic mutants. Similar results were observed when these TIRs were co-expressed with $^{VP16}$*Nb*SAG101b or $^{VP16}$*Nb*PAD4 (Figures 3D and 3E). Immunoblot assays showed that all TIR$^{BD}$ constructs accumulated to similar levels as their NADase mutants *in planta* (Figure S12). Neither L6TIR$^{BD}$ nor L6TIR$^{BD}$ E135A showed association with $^{VP16}$*Nb*EDS1, $^{VP16}$*Nb*SAG101b or $^{VP16}$*Nb*PAD4 in this assay, which is likely because L6TIR is excluded from the nucleus due to its N-terminal Golgi membrane anchor.[19] Nuclear localization of the fusion proteins is required for the activation of *Ruby* expression in this assay.[43] Overall, both the split luciferase and plant two-hybrid assays supported the physical association of plant TIRs with individual EDS1 family members.

## TIR domains interact with the *Nb*EDS1/*Nb*SAG101 complex in yeast

The Co-IP, split-luciferase, and plant two-hybrid assay results above show that plant TIRs can associate with individual EDS1 family proteins *in planta*. However, yeast two-hybrid assays failed to detect interactions between any of these TIR-EDS1 family protein combinations, except for *Nb*EDS1-BD and SNC1TIR-AD (Figures S13A and S13B). On the other hand, interactions between *Nb*EDS1, *Nb*SAG101b, and *Nb*PAD4 and their respective LLD but not EP domains were detected (Figure S13C), consistent with previous reports that EDS1 heterocomplexes are determined mainly by the N-terminal domains of EDS1 family proteins.[25] Because the EDS1 family proteins function as heterodimers, we also tested for interactions of TIRs with the *Nb*EDS1/SAG101b complex in a yeast three-hybrid (Y3H) assay, in which the BD- and AD-fused bait and prey proteins are co-expressed with a third "free" protein (without AD or BD fusion). Unexpectedly, co-expression of *NbEDS1*-BD with a free *NbSAG101b* or *NbPAD4* activated yeast *HIS3* reporter gene expression allowing yeast to grow on media lacking histidine (Figure S14), and this was dependent on the interaction since it did not occur upon co-expression with free *NbSAG101b*-LLVV or *NbPAD4*-VLI mutant proteins. However, co-expression of *NbSAG101b-BD* with free *NbEDS1* did not activate the reporter gene (Figure S14). Thus, Y3H

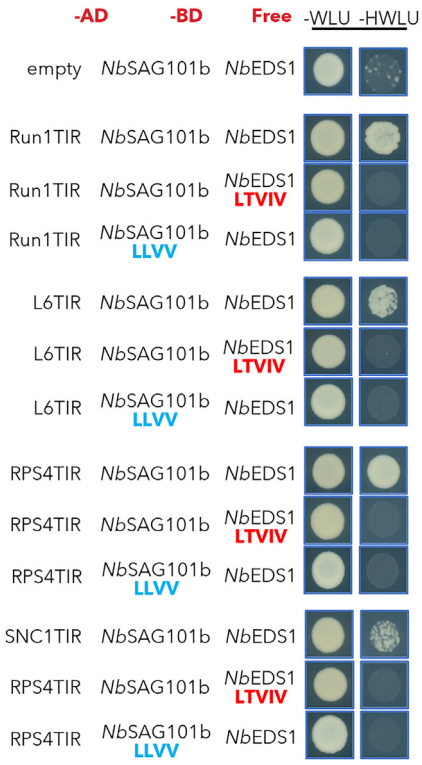


**Figure 4. Plant TIRs interact with the *N. benthamiana* EDS1-SAG101b heterodimer in yeast**

Activation of *HIS3* reporter gene expression in yeast when *Nb*SAG101b-BD plus TIRs-AD were co-expressed with free *Nb*EDS1. The selection for GAL4 activation domain (AD) constructs is leucine (L), for GAL4 binding domain (BD) constructs is -tryptophan (W) and the selection for the construct expressing free proteins in yeast is -uracil. Pictures were taken after 3 days of growth at 30°C.

assays were conducted using yeast cells co-transformed with TIR-AD fusions and *Nb*SAG101b-BD along with free *Nb*EDS1 (Figure 4). This combination led to the activation of the *HIS3* reporter gene and the growth of yeast on histidine selection media for all four TIR domains tested (Run1TIR, L6TIR, RPS4TIR and SNC1TIR). However, mutation of the EDS1 heterodimer interaction surfaces (*Nb*EDS1-LTVIV or *Nb*SAG101b-LLVV) abolished these three-hybrid interactions. This indicates that in yeast, these plant TIR domains preferentially interact directly with the *Nb*EDS1-*Nb*SAG101b heterodimer, rather than the individual proteins as observed *in planta*. Immunoblot analysis showed all the protein fusions were expressed in yeast (Figure S15).

## *Nb*NRG1 associates with *Nb*SAG101b in competition with *Nb*EDS1

Because the helper NLR *Nb*NRG1 acts downstream of TIR-EDS1/SAG101b, we also tested physical associations between this protein and the *Nb*EDS1 family by Co-IP. *Nb*NRG1-3xHA was co-immunoprecipitated by *Nb*SAG101b-YFP, while only small amounts were detected after pull-down by *Nb*PAD4-YFP and *Nb*SAG101a-YFP, and none was detected with *Nb*EDS1-YFP (Figure 5A). No associations were detected between *Nb*ADR1 and *Nb*EDS1 family proteins under these conditions. *Nb*SAG101b could form a trimeric complex with *Nb*EDS1 and *Nb*NRG1, or two mutually exclusive *Nb*EDS1-*Nb*SAG101b and *Nb*SAG101b-*Nb*NRG1 dimeric complexes. To discriminate between these possibilities, we performed three-way Co-IP assays in *eds1* mutant plants using *Nb*SAG101b-YFP as bait to pull down *Nb*NRG1-3xHA in the presence or absence of *Nb*EDS1-3Myc. As shown in Figure 5B, *Nb*SAG101b-YFP co-immunoprecipitates with *Nb*NRG1 in the absence of *Nb*EDS1, but this association is substantially reduced when *Nb*EDS1-3Myc is co-expressed. On the other hand, co-expression of the *Nb*EDS1-3Myc-LTVIV variant, which cannot interact with *Nb*SAG101b, did not affect the association between *Nb*SAG101b and *Nb*NRG1. Likewise, co-expression of *Nb*EDS1-3Myc did not affect the association between *Nb*NRG1 and the *Nb*SAG101b-LLVV variant, which cannot interact with *Nb*EDS1. As expected, *Nb*SAG101b-YFP pulled down *Nb*EDS1-3Myc, but not *Nb*EDS1-3Myc-LTVIV, while *Nb*SAG101b-YFP-LLVV did not pull down *Nb*EDS1-3Myc. Thus, the presence of *Nb*EDS1 inhibits the association between *Nb*SAG101b and *Nb*NRG1 and this is dependent on its ability to form a heterocomplex with *Nb*SAG101. As a further test for a possible trimeric complex, Co-IP assays were carried out in *pss* mutant plants using *Nb*EDS1-YFP as bait to pull down *Nb*NRG1-3xHA and/or *Nb*SAG101b-3Myc. As previously, *Nb*EDS1-YFP did not pull down *Nb*NRG1-3xHA but did pull down *Nb*SAG101b-3Myc. Neither the presence of *Nb*SAG101b-3Myc or *Nb*SAG101b-3Myc LLVV variant could mediate *Nb*EDS1-YFP to pull down *Nb*NRG1-3xHA (Figure 5C). These data suggest that the *Nb*EDS1-*Nb*SAG101b and *Nb*SAG101b-*Nb*NRG1 complexes detected in these assays are independent and mutually exclusive, with the *Nb*EDS1-*Nb*SAG101b interaction the favored form, since the expression of *Nb*EDS1 had a strong effect on inhibiting the *Nb*SAG101b-*Nb*NRG1 association, while the expression of NRG1 had only a weak effect in reducing the EDS1-SAG101b interaction. Thus, the *Nb*EDS1-*Nb*SAG101b heterodimer likely predominates in native unchallenged cells in the absence of TIR-mediated signaling, with this interaction likely occluding the site in *Nb*SAG101b that mediates association with *Nb*NRG1.

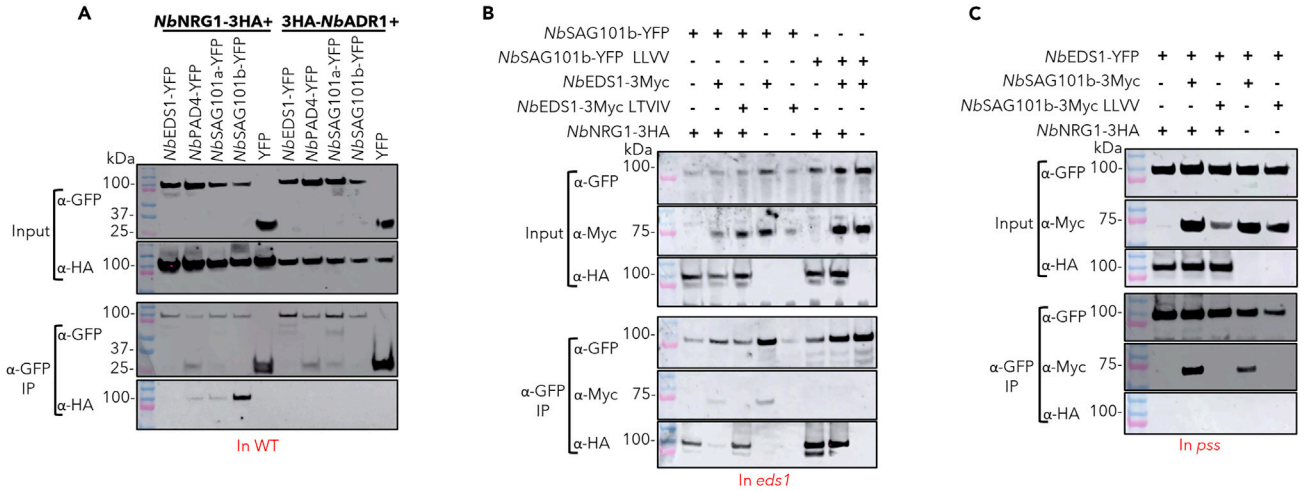


**Figure 5. Interaction of *N. benthamiana* EDS1 family proteins with helper RNLs**

(A) Co-IP experiments between *Nb*EDS1-YFP, *Nb*PAD4-YFP or *Nb*SAG101-YFP with *Nb*NRG1-3xHA or 3xHA-*Nb*ADR1. The indicated protein fusion combinations were expressed transiently in wildtype *N. benthamiana* plants. Tagged proteins were detected in the extract (input) and after immunoprecipitation with anti-GFP beads (IP) by immunoblotting with anti-HA (α-HA) and anti-GFP (α-GFP) antibodies.

(B) Competitive Co-IP testing interactions between *Nb*SAG101b-YFP, *Nb*SAG101b-YFP LLVV and *Nb*NRG1-3xHA, *Nb*EDS1-3Myc and *Nb*EDS1-3Myc LTVIV. Protein combinations indicated above the blot (+ construct agro-infiltrated; - non agro-infiltrated construct) was expressed in *eds1* plants.

(C) Competitive Co-IP for interactions between *Nb*EDS1-YFP with *Nb*NRG1-3xHA and *Nb*SAG101-3Myc and *Nb*SAG101-3Myc LLVV. The indicated protein fusion combinations were expressed transiently in *pss* plants.

## The EP domain of *Nb*SAG101b and the NB-LRR region of *Nb*NRG1 mediate their association

To further characterize, the *Nb*NRG1-*Nb*SAG101b interaction, we tested various subdomains of each protein. The EP domain of *Nb*SAG101b showed stronger association with *Nb*NRG1 in Co-IP assays than the LLD domain, albeit weaker than full-length *Nb*SAG101b (Figure 6A). To further test this, the LLD and EP domains of *Nb*SAG101b were swapped with the corresponding domains from *Nb*PAD4 and *Nb*SAG101a to generate four chimeric proteins: NSb:CP, NSb:CSa, NP:CSb, and NSa:CSb (Figure S16). The chimeric proteins were first tested for interaction with *Nb*EDS1. All four chimeras showed strong interactions with *Nb*EDS1 similar to the wildtype *Nb*PAD4 and *Nb*SAG101 proteins (Figure 6B), confirming that they can form heterocomplexes with *Nb*EDS1. However, only the wildtype *Nb*SAG101b and chimeras containing the *Nb*SAG101b EP domain, NP:CSb and NSa:CSb, could co-immunoprecipitate *Nb*NRG1-3xHA, whereas *Nb*SAG101a, *Nb*PAD4, *Nb*EDS1 and chimeras with either the *Nb*PAD4 or *Nb*SAG101a EP domains (NSb:CP and NSb:CSa) failed to interact with *Nb*NRG1 (Figure 6C). The NP:CSb and NSa:CSb chimeric proteins, which both interacted with *Nb*NRG1, also recovered cell death induction by Run1TIR-YFP in the *N. benthamiana pss* line (Figure 6D). However, the inverse fusion proteins lacking the SAG101b EP domain, NSb:CP and NSb:CSa, did not complement cell death signaling in this background. Thus, the EP domain of *Nb*SAG101b determines the specificity of interaction with *Nb*NRG1 and the ability to activate TIR-induced cell death in *N. benthamiana*.

We also tested the association between *Nb*SAG101b and different domains of *Nb*NRG1 (Figure 7A). *Nb*SAG101b-YFP could pull down full-length *Nb*NRG1-3xHA as well as the NB (aa 219–609), LRR (aa 604–850), and NB-LRR (aa 219–850) fragments, but not the CC (aa 1–182) domain. Similarly, all of the NRG1 domain fragments except for the CC domain interacted with the *Nb*SAG101b chimeric proteins NSa:CSb and NP:CSb (Figure 7B). Surprisingly, the separated NB and LRR domains of *Nb*NRG1 each co-immunoprecipitated with all members of the *Nb*EDS1 family, including *Nb*PAD4, *Nb*SAG101a and the four chimeric proteins, although the association with *Nb*EDS1 was weak (Figures 7C and 7D). However, the NB-LRR fragment of NRG1 only co-immunoprecipitated with *Nb*SAG101b and the NSa:CSb and NP:CSb chimeras (Figure 7E), similar to the full-length NRG1 protein. Thus, it appears that the combination of the NB and LRR domains confers the specificity of NRG1 for *Nb*SAG101b.

## DISCUSSION

EDS1 forms mutually exclusive heterocomplexes with PAD4 or SAG101 and acts downstream of TIR-NLR immune receptors to transduce immune signals to the downstream helper NLRs NRG1 and ADR1.[25,26,28,32] Some TIR-NLR receptors have been reported to require only *Nb*EDS1, *Nb*SAG101b and *Nb*NRG1 for cell death in *N. benthamiana*, but not *Nb*SAG101a or *Nb*ADR1.[27,31,34] Here we showed that the *Nb*EDS1-*Nb*SAG101b-*Nb*NRG1 signaling module in *N. benthamiana* is commonly required for cell death mediated by a broader set of TIR domains from diverse plant species expressed in different cell death activating contexts (Figures 1 and S1–S6). In contrast, *Nb*PAD4 and *Nb*SAG101a do not contribute to cell death induction despite forming heterocomplexes with *Nb*EDS1. An exception was observed for cell death induced by the RPS4 TIR domain, which was reduced but not fully abolished in all of the mutant lines. This residual activity

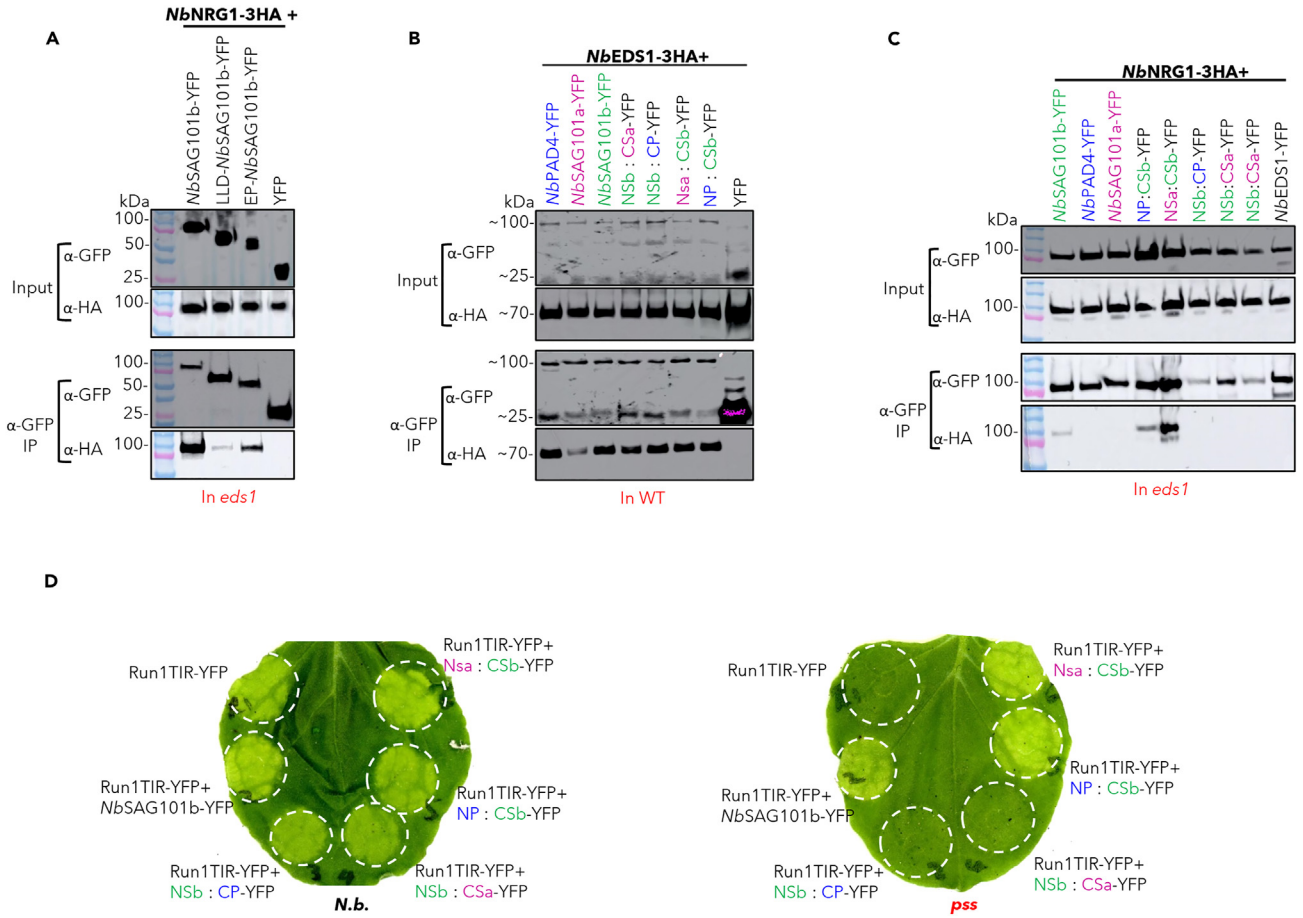


**Figure 6. Functional analysis of EDS1-family chimeric proteins**

(A) Co-IP assays between *Nb*SAG101b, the N-terminal lipase-like (LLD) domain of *Nb*SAG101b and the C-terminal EP (EP) domain of *Nb*SAG101b (fused to YFP tags) with *Nb*NRG1-3xHA.

(B and C) Co-IP assays between *Nb*EDS1-3xHA and *Nb*NRG1-3xHA with *Nb*SAG101b, *Nb*SAG101a, *Nb*PAD4, and the chimeric proteins.

(D) Complementation of Run1TIR-YFP cell death by *Nb*SAG101b and the domain swap chimeric proteins in *pss* mutant plants. The agrobacterium concentration was OD600 = 0.5. All combinations caused similar cell death phenotypes in wildtype *N. benthamiana*.

was observed in a total of 171 out of 227 infiltrations performed with constructs containing the RPS4-TIR across the four mutant backgrounds and was dependent on TIR catalytic activity and oligomerization, so the RPS4 TIR may partially bypass *Nb*EDS1/*Nb*SAG101/*Nb*NRG1 to signal via an unknown mechanism(s).

## TIR domains interact physically with EDS1 family proteins

The *Arabidopsis* full-length TIR-NLRs RPS4, RPS6, and SNC1 have been reported to associate with *At*EDS1 in Co-IP experiments.[44–47] We found that the TIR domains of L6, Run1, RPS4, and SNC1 physically associated with *Nb*EDS1, *Nb*PAD4, and *Nb*SAG101 in Co-IP experiments (Figure 2), and this was confirmed by *in planta* two-hybrid assays and also by split-LUC assays for Run1TIR and L6TIR (Figures 3, S11, and S12). Similar results were observed for these TIR domains with the *Arabidopsis* EDS1 family proteins (Figure S10). The observed interactions of TIR domains from flax, grapevine and Arabidopsis with EDS1 family proteins from *N. benthamiana* and Arabidopsis suggestions that this is a conserved feature of TIR-EDS1 signaling across diverse plants. In these *in planta* experiments, TIR association with *Nb*EDS1 was independent of *Nb*PAD4 and *Nb*SAG101, and association with *Nb*PAD4 or *Nb*SAG101 was independent of *Nb*EDS1. However, in yeast two- and three-hybrid assays (Figure 4), TIR interactions were detected only with *Nb*EDS1 and *Nb*SAG101 complexes, but not with the individual proteins, and were dependent on the *Nb*EDS1-*Nb*SAG101 interaction. In the *in planta* Co-IP assays, co-expression of *Nb*SAG101 did not affect the TIR domain association with *Nb*EDS1 (Figure S9C), suggesting that the two interactions are not mutually exclusive and could occur simultaneously. This may be required for detection in the yeast assay system due to its different physical parameters compared to Co-IP. Additional plant proteins may facilitate TIR association with individual EDS1 family proteins when expressed *in planta*, while the yeast assay involves direct interactions in the absence of other plant proteins. Moreover, mutations that affect L6TIR oligomerization also did not affect its association with *Nb*EDS1 (Figure S9E), suggesting that both monomeric and oligomeric TIR domains could interact with EDS1 family proteins.

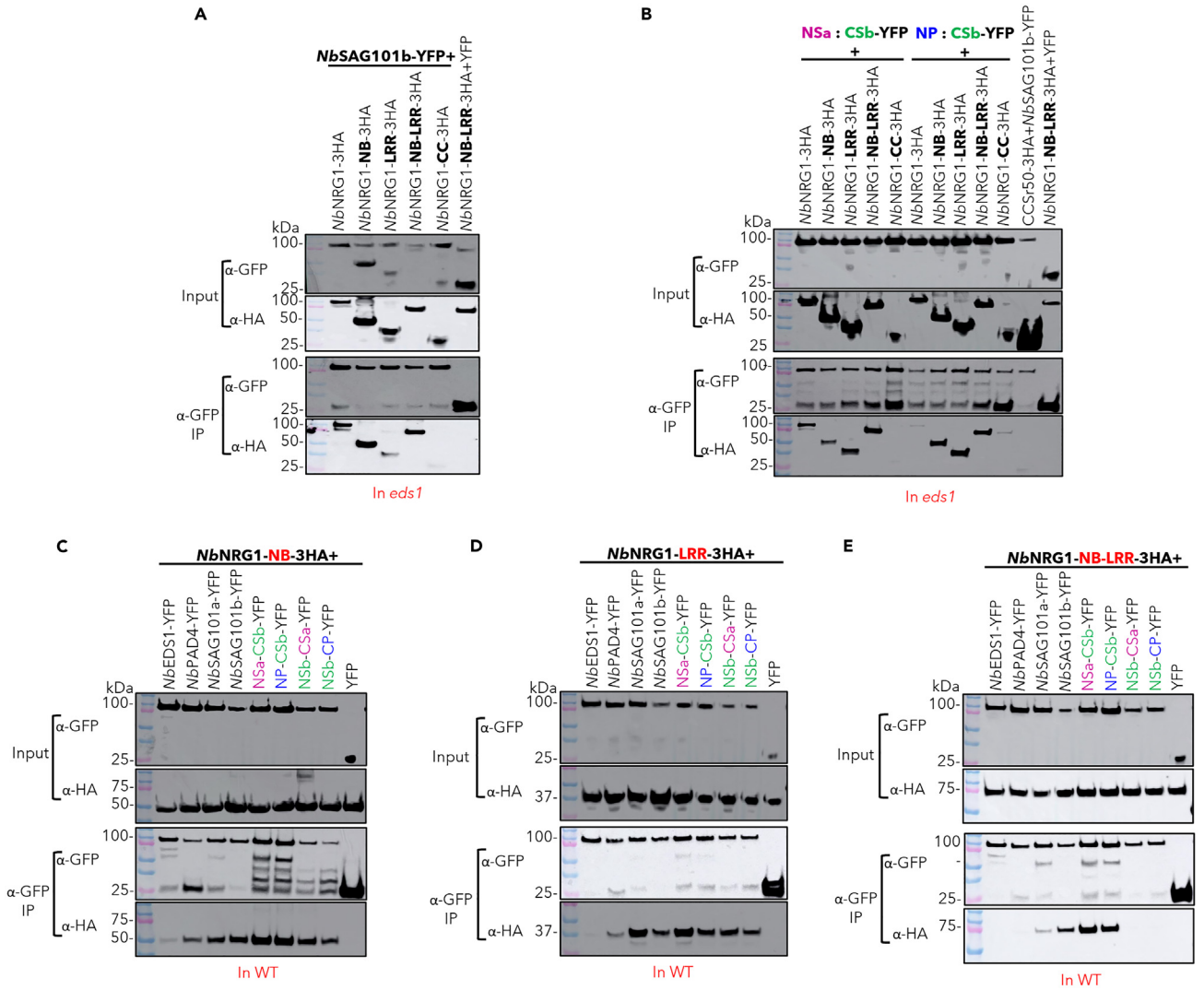


**Figure 7. Interactions between *Nb*NRG1 domains and EDS1 family proteins**

(A and B) Co-IP assays between *Nb*NRG1 and its subdomains fused to a 3xHA tag in combination with *Nb*SAG101b chimeric proteins NSa:CSb and NP:CSb fused to a YFP tag.

(C–E) Co-IP assays of *Nb*NRG1 domains NB, LRR, and NB-LRR in combination with *Nb*EDS1 family and chimeric proteins.

Run1TIR associates primarily with the LLD domain fragments of *Nb*EDS1, *Nb*PAD4, and *Nb*SAG101b rather than their EP domain fragments (Figures 2E and S11D). Given the tetrameric structure of the activated TIR domains in RPP1 and Roq1 resistosomes,[20,21] and the stable heterodimers formed by EDS1 family members, it is possible that both partners of an EDS1/SAG101b heterodimer could interact directly with two different TIR domain subunits of an activated TIR-NLR resistosome (Figure S17). While monomeric TIR domains would be capable of interacting with either the EDS1 or SAG101 subunits of the EDS1-SAG101 heterocomplex, only the tetramer is catalytically active and able to interact with both subunits. Interaction of EDS1 heterodimers with inactive monomeric TIR domains may facilitate their recruitment by activated resistosomes to allow substrate-mediated signaling. However, it is also possible that the TIR domains of inactive TIR-NLR monomers are not available for interaction with EDS1 family proteins.

The pRib-AMP/ADP and ADPr-ATP/di-ADPR products detected in TIR-activated EDS1-PAD4 and EDS1-SAG101 complexes were not detected as free molecules *in planta*,[35,36] nor in *in vitro* enzyme assays.[14,15] Direct interaction between TIR domains and EDS1 family heterodimers may help explain the discrepancy between these results in several ways. Firstly, given the instability or low abundance of the pRib-AMP/ADP and ADPr-ATP/di-ADPR products *in planta*, physical interaction may be required to allow efficient transfer of these molecular signals from activated TIR domains to EDS1 protein complexes. Secondly, the enzymatic activity of the TIR domains may be altered when in complex with EDS1 heterodimers such that these signaling molecules become the favored products in preference to v-cADPR observed in *in vitro* assays of isolated TIR domains. Thirdly, it is possible that the activated TIR enzymes act on a substrate pre-bound to the EDS1

complexes. These hypotheses are not mutually exclusive and may all apply. Interestingly, the TIR NADase catalytic site mutations showed stronger association with *Nb*EDS1 family proteins than did the wildtype proteins in several assays. A possible explanation is that these mutations enhance the protein complex stability by preventing loss of a co-bound substrate or dissociation of the TIR from the complex after the detection of the catalytic products by the EDS1 heterodimer.

## NRG1 interacts with SAG101b through the EP domain

We found that *Nb*NRG1 associated with *Nb*SAG101b in CoIP experiments but not with *Nb*PAD4 or *Nb*SAG101a (Figures 5A and 5B). This is consistent with the requirement for the *Nb*EDS1/*Nb*SAG101b/*Nb*NRG1 signaling module for TIR-NLR signaling in *N. benthamiana*, and the specific role of NRG1 downstream of EDS/SAG101 but not EDS1/PAD4.[39] Although *Nb*NRG1 was previously reported to associate with *Nb*EDS1 by Co-IP,[27] interactions with other EDS1 family members were not previously tested. However, we did not detect any association between *Nb*EDS1 and *Nb*NRG1. This could be due to the higher expression levels of *Nb*NRG1 in the Qi et al.[27] study, which showed very strong autoactivity. The *Nb*EDS1/*Nb*SAG101b and *Nb*NRG1/*Nb*SAG101b interactions appeared to be mutually exclusive, since *Nb*EDS1 effectively competed with *Nb*NRG1 to form complexes with *Nb*SAG101b and this competition did not occur with the non-interacting mutants *Nb*EDS1-LTVIV or *Nb*SAG101b-LLVV (Figure 5C). Thus, under normal cellular conditions, *Nb*EDS1 likely sequesters *Nb*SAG101b and prevents interaction with *Nb*NRG1 in the absence of TIR activation. *Nb*NRG1 associates preferentially with the EP domain of *Nb*SAG101b, and domain swaps between *Nb*SAG101b and *Nb*PAD4 and the non-functional *Nb*SAG101a revealed that the EP domain controls this specificity as well as the ability to complement cell death signaling (Figure 6). These conclusions are consistent with previous work by Gantner et al.[34] who tested similar domain swaps between the tomato *Sl*SAG101a and *Sl*SAG101b proteins and found that the C-terminal domain of *Sl*SAG101b was sufficient to restore activity to the non-functional *Sl*SAG101a. Similarly, chimeric proteins between Arabidopsis PAD4 and SAG101 revealed that the *At*SAG101 EP domain is necessary for Roq1-induced cell death in *N. benthamiana*.[31,34]

It is important to note that the association between *Nb*NRG1 and *Nb*SAG101b observed here occurs in the absence of cell death signaling, which requires TIR domain enzymatic activity. Thus, while these associations may define the specificity of the *Nb*NRG1 interaction with *Nb*SAG101b, activation of *Nb*NRG1 requires the presence of the activated *Nb*EDS1-*Nb*SAG101b complex bound to ADPr-ATP. Indeed, binding of di-ADPR or ADPr-ATP by the *At*EDS1-*At*SAG101 heterodimer induces allosteric rotation of the *At*SAG101 EP domain, which is proposed to trigger immunity activation by promoting interaction with *At*NRG1A.[35,36] Thus, a likely scenario is that this alteration in the *Nb*EDS1/*Nb*SAG101b complex after TIR activation leads to the exposure of a binding surface of the *Nb*SAG101b EP that interacts directly with *Nb*NRG1. This surface would be exposed in the free monomeric *Nb*SAG101b expressed in the Co-IP assays here but would not be available in the pre-activation *Nb*EDS1/*Nb*SAG101 complex present under normal cellular conditions, explaining the competition between EDS1 and NbNRG1 for SAG101b (Figure 5). Structural data on ZAR1 and Sr35 resistosomes revealed that the ligand bound in the active state would sterically clash with the NB domain position in the inactive state, thereby promoting resistosome assembly.[8,10] Monomeric *Nb*SAG101b may bind to inactive *Nb*NRG1 without causing such a steric clash, while binding of the larger *Nb*EDS1/*Nb*SAG101 complex would promote the formation of an active NRG1 resistosome. These possibilities are consistent with observations that *At*NRG1 associates with *At*EDS1 and *At*SAG101 to form a functional signaling complex in the immune-activated state[31,48] and upon the activation of PTI and TIR-NLR mediated ETI, a small proportion of *At*NRG1 forms stable resistosomes with *At*EDS1 and *At*SAG101.[37]

While *Nb*NRG1 specifically associates with *Nb*SAG101b in Co-IP, no associations were detected between *Nb*ADR1 and its immune partner *Nb*PAD4 and other *Nb*EDS1 family proteins in this study. This may explain why the *Nb*EDS1-*Nb*SAG101b-*Nb*NRG1 module is required for cell death mediated by TIR-NLRs, but *Nb*ADR1 has not been reported to be involved in ETI responses. However, a recent study reported that EDS1/PAD4 and ADR1 are required in both *N. benthamiana* and *A. thaliana* for stomatal immunity induced by flg22 or bacteria, suggesting a functional role of this module in immunity separate to cell death induction.[49] It is not clear whether TIR signaling is involved in these stomatal immune responses, or whether this pathway is restricted to guard cells.

An unexpected observation here was that the moderately high expression of *Nb*NRG1 could inhibit TIR-NLR mediated cell death in *N. benthamiana* (Figure S6B). Given that *Nb*NRG1 associates with *Nb*SAG101b in competition with *Nb*EDS1, we hypothesize that the overexpression of *Nb*NRG1 may sequester *Nb*SAG101b away from the *Nb*EDS1/*Nb*SAG101b complex required to transduce the cell death signal from the TIR proteins to *Nb*NRG1. A recent discovery showed that the *Arabidopsis* NRG1C, an N-terminally truncated member of the NRG1 family, inhibits TIR-NLR induced cell death by antagonizing the function of full-length NRG1A and NRG1B, possibly by interfering with the EDS1-SAG101-NRG1A/B axis.[50] Interestingly, the NB, LRR and the combined NB-LRR domains of *Nb*NRG1 all associated with *Nb*SAG101b and functional chimeras containing its EP domain (Figure 7). However, the isolated NB and LRR domains of *Nb*NRG1 showed a loss of specificity in that they could also interact with all the *Nb*EDS1 family and chimeric proteins. Thus, it seems that the NB and LRR domains act together to provide the specificity of *Nb*NRG1 for *Nb*SAG101b.

## Model for signal transduction in TIR-EDS1/SAG101b/NRG1 pathway

Figure S17 shows a hypothetical model of TIR signaling events leading to the activation of *Nb*NRG1. Effector recognition leads to a TIR-NLR forming a tetrameric resistosome which activates the TIR domain catalytic activity.[15,20,21,35,36] The TIR domain tetramers interact with the LLD domains of EDS1 family heterodimers, potentially involving multiple interactions between different subunits of both complexes. This physical interaction may allow efficient transfer of signaling molecules, alter TIR enzymatic activity and/or provide access to a substrate pre-bound to the EDS1 protein complex. After the detection of the TIR-derived molecular signal, the EDS1/SAG101 complex undergoes a conformational shift allowing the EP domain of SAG101 to interact with both the NB and LRR domains of NRG1. This interaction results in the activation of the

*Nb*NRG1 protein likely through oligomerisation into a resistosome structure and formation of a $Ca^{2+}$ permeable cation channel.[37,38] There is conflicting evidence as to whether EDS1/SAG101b is present in the active NRG1 resistosome.[37,51]

### Limitations of the study

The association between TIR domains and EDS1 proteins described here were only tested for isolated TIR domains and not in the context of full-length TIR-NLRs. Although the isolated TIR domains appear to associate with EDS proteins constitutively and independently of oligomerization or catalytic activity, in the context of a full-length TIR-NLR in the inactive state the TIR domain interaction surfaces may not be exposed, and EDS1 complex interaction may be dependent upon the activation of the TIR-NLR. We have not tested whether TIR-NLR activation induces an association of the full-length proteins with EDS1. Similarly, the specific association observed between *Nb*NRG1 and *Nb*SAG101 was detected in the absence of TIR-activated signaling. While informative for defining the basis of specificity of NRG1 for SAG101, this interaction is not sufficient for the activation of NRG1 signaling.

## STAR★METHODS

Detailed methods are provided in the online version of this paper and include the following:

- KEY RESOURCES TABLE
- RESOURCE AVAILABILITY
  - Lead contact
  - Materials availability
  - Data and code availability
- EXPERIMENTAL MODEL AND STUDY PARTICIPANT DETAILS
  - Plant growth
  - Bacterial growth
- METHOD DETAILS
  - Generation of constructs
  - Transient expression in *N. benthamiana*
  - Yeast two-hybrid and yeast three-hybrid assays
  - Split-luciferase and plant two-hybrid assays
  - Protein extraction, immunoblot, and coimmunoprecipitation
- QUANTIFICATION AND STATISTICAL ANALYSIS

## SUPPLEMENTAL INFORMATION

Supplemental information can be found online at https://doi.org/10.1016/j.isci.2024.108817.

## ACKNOWLEDGMENTS

The mutant lines of *N. benthamiana* were kindly provided by B. Staskawicz (*eds1*) and J. Stuttmann (*eds1/pad4*, *pad4/sag101a/sag101b* and *nrg1*). JC was supported by a Chinese Scholarship Council (CSC) postgraduate fellowship.

## AUTHOR CONTRIBUTIONS

JC conducted experimental work and drafted the article. PND, JPR, and MB conceived the study. All authors contributed to data analysis and interpretation and article writing.

## DECLARATION OF INTERESTS

The authors declare no competing interests.

Received: August 20, 2023
Revised: November 9, 2023
Accepted: January 2, 2024
Published: January 24, 2024

## REFERENCES

1. Jones, J.D.G., and Dangl, J.L. (2006). The plant immune system. Nature *444*, 323–329.
2. Dodds, P.N., and Rathjen, J.P. (2010). Plant immunity: towards an integrated view of plant-pathogen interactions. Nat. Rev. Genet. *11*, 539–548.
3. Ngou, B.P.M., Ding, P., and Jones, J.D.G. (2022). Thirty years of resistance: Zig-zag through the plant immune system. Plant Cell *34*, 1447–1478.
4. Qi, D., and Innes, R.W. (2013). Recent Advances in Plant NLR Structure, Function,

Localization, and Signaling. Front. Immunol. *4*, 348.
5. Zhang, X., Dodds, P.N., and Bernoux, M. (2017). What Do We Know About NOD-Like Receptors in Plant Immunity? Annu. Rev. Phytopathol. *55*, 205–229.
6. Chen, J., Zhang, X., Rathjen, J.P., and Dodds, P.N. (2022). Direct recognition of pathogen effectors by plant NLR immune receptors and downstream signalling. Essays Biochem. *66*, 471–483.
7. Wang, J., Hu, M., Wang, J., Qi, J., Han, Z., Wang, G., Qi, Y., Wang, H.W., Zhou, J.M., and Chai, J. (2019). Reconstitution and structure of a plant NLR resistosome conferring immunity. Science *364*, eaav5870.
8. Wang, J., Wang, J., Hu, M., Wu, S., Qi, J., Wang, G., Han, Z., Qi, Y., Gao, N., Wang, H.W., et al. (2019). Ligand-triggered allosteric ADP release primes a plant NLR complex. Science *364*, eaav5868.
9. Bi, M.S., Nan Li, Y.L., Dang, S., Xu, J., Hu, M., Wang, J., Zou, M., Yanan Deng, Q.L., Huang, S., Li, J., et al. (2021). The ZAR1 resistosome is a calcium-permeable channel triggering plant immune signaling. Cell *184*, 3528–3541.e12.
10. Förderer, A., Li, E., Lawson, A.W., Deng, Y.N., Sun, Y., Logemann, E., Zhang, X., Wen, J., Han, Z., Chang, J., et al. (2022). A wheat resistosome defines common principles of immune receptor channels. Nature *610*, 532–539.
11. Bernoux, M., Ve, T., Williams, S., Warren, C., Hatters, D., Valkov, E., Zhang, X., Ellis, J.G., Kobe, B., and Dodds, P.N. (2011). Structural and functional analysis of a plant resistance protein TIR domain reveals interfaces for self-association, signaling, and autoregulation. Cell Host Microbe *9*, 200–211.
12. Williams, S.J., Sohn, K.H., Wan, L., Bernoux, M., Sarris, P.F., Segonzac, C., Ve, T., Ma, Y., Saucet, S.B., Ericsson, D.J., et al. (2014). Structural basis for assembly and function of a heterodimeric plant immune receptor. Science *344*, 299–303.
13. Zhang, X., Bernoux, M., Bentham, A.R., Newman, T.E., Ve, T., Casey, L.W., Raaymakers, T.M., Hu, J., Croll, T.I., Schreiber, K.J., et al. (2017). Multiple functional self-association interfaces in plant TIR domains. Proc. Natl. Acad. Sci. USA *114*, E2046–E2052.
14. Wan, L., Essuman, K., Anderson, R.G., Sasaki, Y., Monteiro, F., Chung, E.H., Osborne Nishimura, E., DiAntonio, A., Milbrandt, J., Dangl, J.L., and Nishimura, M.T. (2019). TIR domains of plant immune receptors are NAD(+)-cleaving enzymes that promote cell death. Science *365*, 799–803.
15. Horsefield, S., Burdett, H., Zhang, X., Manik, M.K., Shi, Y., Chen, J., Qi, T., Gilley, J., Lai, J.S., Rank, M.X., et al. (2019). NAD(+) cleavage activity by animal and plant TIR domains in cell death pathways. Science *365*, 793–799.
16. Duxbury, Z., Wang, S., MacKenzie, C.I., Tenthorey, J.L., Zhang, X., Huh, S.U., Hu, L., Hill, L., Ngou, P.M., Ding, P., et al. (2020). Induced proximity of a TIR signaling domain on a plant-mammalian NLR chimera activates defense in plants. Proc. Natl. Acad. Sci. USA *117*, 18832–18839.
17. Kofoed, E.M., and Vance, R.E. (2011). Innate immune recognition of bacterial ligands by NAIPs determines inflammasome specificity. Nature *477*, 592–595.
18. Zhao, Y., Yang, J., Shi, J., Gong, Y.N., Lu, Q., Xu, H., Liu, L., and Shao, F. (2011). The NLRC4 inflammasome receptors for bacterial flagellin and type III secretion apparatus. Nature *477*, 596–600.
19. Bernoux, M., Chen, J., Zhang, X., Newell, K., Hu, J., Deslandes, L., and Dodds, P. (2023). Subcellular localization requirements and specificities for plant immune receptor Toll-interleukin-1 receptor signaling. Plant J. *114*, 1319–1337.
20. Martin, R., Qi, T., Zhang, H., Liu, F., King, M., Toth, C., Nogales, E., and Staskawicz, B.J. (2020). Structure of the activated ROQ1 resistosome directly recognizing the pathogen effector XopQ. Science *370*, eabd9993.
21. Ma, S., Lapin, D., Liu, L., Sun, Y., Song, W., Zhang, X., Logemann, E., Yu, D., Wang, J., Jirschitzka, J., et al. (2020). Direct pathogen-induced assembly of an NLR immune receptor complex to form a holoenzyme. Science *370*, eabe3069.
22. Wiermer, M., Feys, B.J., and Parker, J.E. (2005). Plant immunity: the EDS1 regulatory node. Curr. Opin. Plant Biol. *8*, 383–389.
23. Feys, B.J., Wiermer, M., Bhat, R.A., Moisan, L.J., Medina-Escobar, N., Neu, C., Cabral, A., and Parker, J.E. (2005). Arabidopsis SENESCENCE-ASSOCIATED GENE101 stabilizes and signals within an ENHANCED DISEASE SUSCEPTIBILITY1 complex in plant innate immunity. Plant Cell *17*, 2601–2613.
24. García, A.V., Blanvillain-Baufumé, S., Huibers, R.P., Wiermer, M., Li, G., Gobbato, E., Rietz, S., and Parker, J.E. (2010). Balanced nuclear and cytoplasmic activities of EDS1 are required for a complete plant innate immune response. PLoS Pathog. *6*, e1000970.
25. Wagner, S., Stuttmann, J., Rietz, S., Guerois, R., Brunstein, E., Bautor, J., Niefind, K., and Parker, J.E. (2013). Structural basis for signaling by exclusive EDS1 heteromeric complexes with SAG101 or PAD4 in plant innate immunity. Cell Host Microbe *14*, 619–630.
26. Castel, B., Ngou, P.M., Cevik, V., Redkar, A., Kim, D.S., Yang, Y., Ding, P., and Jones, J.D.G. (2019). Diverse NLR immune receptors activate defence via the RPW8-NLR NRG1. New Phytol. *222*, 966–980.
27. Qi, T., Seong, K., Thomazella, D.P.T., Kim, J.R., Pham, J., Seo, E., Cho, M.J., Schultink, A., and Staskawicz, B.J. (2018). NRG1 functions downstream of EDS1 to regulate TIR-NLR-mediated plant immunity in Nicotiana benthamiana. Proc. Natl. Acad. Sci. USA *115*, E10979–E10987.
28. Wu, Z., Li, M., Dong, O.X., Xia, S., Liang, W., Bao, Y., Wasteneys, G., and Li, X. (2019). Differential regulation of TNL-mediated immune signaling by redundant helper CNLs. New Phytol. *222*, 938–953.
29. Jubic, L.M., Saile, S., Furzer, O.J., El Kasmi, F., and Dangl, J.L. (2019). Help wanted: helper NLRs and plant immune responses. Curr. Opin. Plant Biol. *50*, 82–94.
30. Collier, S.M., Hamel, L.P., and Moffett, P. (2011). Cell death mediated by the N-terminal domains of a unique and highly conserved class of NB-LRR protein. Mol. Plant Microbe Interact. *24*, 918–931.
31. Lapin, D., Kovacova, V., Sun, X., Dongus, J.A., Bhandari, D., von Born, P., Bautor, J., Guarneri, N., Rzemieniewski, J., Stuttmann, J., et al. (2019). A Coevolved EDS1-SAG101-NRG1 Module Mediates Cell Death Signaling by TIR-Domain Immune Receptors. Plant Cell *31*, 2430–2455.
32. Rietz, S., Stamm, A., Malonek, S., Wagner, S., Becker, D., Medina-Escobar, N., Corina Vlot, A., Feys, B.J., Niefind, K., and Parker, J.E. (2011). Different roles of Enhanced Disease Susceptibility1 (EDS1) bound to and dissociated from Phytoalexin Deficient4 (PAD4) in Arabidopsis immunity. New Phytol. *191*, 107–119.
33. Bhandari, D.D., Lapin, D., Kracher, B., von Born, P., Bautor, J., Niefind, K., and Parker, J.E. (2019). An EDS1 heterodimer signalling surface enforces timely reprogramming of immunity genes in Arabidopsis. Nat. Commun. *10*, 772.
34. Gantner, J., Ordon, J., Kretschmer, C., Guerois, R., and Stuttmann, J. (2019). An EDS1-SAG101 Complex is Essential for TNL-mediated Immunity in Nicotiana benthamiana. Plant Cell *31*, 2456–2474.
35. Jia, A., Huang, S., Song, W., Wang, J., Meng, Y., Sun, Y., Xu, L., Laessle, H., Jirschitzka, J., Hou, J., et al. (2022). TIR-catalyzed ADP-ribosylation reactions produce signaling molecules for plant immunity. Science *377*, eabq8180.
36. Huang, S., Jia, A., Song, W., Hessler, G., Meng, Y., Sun, Y., Xu, L., Laessle, H., Jirschitzka, J., Ma, S., et al. (2022). Identification and receptor mechanism of TIR-catalyzed small molecules in plant immunity. Science *377*, eabq3297.
37. Feehan, J.M., Wang, J., Sun, X., Choi, J., Ahn, H.K., Ngou, B.P.M., Parker, J.E., and Jones, J.D.G. (2023). Oligomerization of a plant helper NLR requires cell-surface and intracellular immune receptor activation. Proc. Natl. Acad. Sci. USA *120*, e2210406120.
38. Jacob, P., Kim, N.H., Wu, F., El-Kasmi, F., Chi, Y., Walton, W.G., Furzer, O.J., Lietzan, A.D., Sunil, S., Kempthorn, K., et al. (2021). Plant "helper" immune receptors are Ca(2+)-permeable nonselective cation channels. Science *373*, 420–425.
39. Locci, F., Wang, J., and Parker, J.E. (2023). TIR-domain enzymatic activities at the heart of plant immunity. Curr. Opin. Plant Biol. *74*, 102373.
40. Ordon, J., Martin, P., Erickson, J.L., Ferik, F., Balcke, G., Bonas, U., and Stuttmann, J. (2021). Disentangling cause and consequence: genetic dissection of the DANGEROUS MIX2 risk locus, and activation of the DM2h NLR in autoimmunity. Plant J. *106*, 1008–1023.
41. Peart, J.R., Mestre, P., Lu, R., Malcuit, I., and Baulcombe, D.C. (2005). NRG1, a CC-NB-LRR protein, together with N, a TIR-NB-LRR protein, mediates resistance against tobacco mosaic virus. Curr. Biol. *15*, 968–973.
42. Gehl, C., Kaufholdt, D., Hamisch, D., Bikker, R., Kudla, J., Mendel, R.R., and Hänsch, R. (2011). Quantitative analysis of dynamic protein-protein interactions in planta by a floated-leaf luciferase complementation imaging (FLuCI) assay using binary Gateway vectors. Plant J. *67*, 542–553.
43. Chen, J., Luo, M., Hands, P., Rolland, V., Zhang, J., Li, Z., Outram, M., Dodds, P., and Ayliffe, M. (2023). A split GAL4 RUBY assay for visual in planta detection of protein-protein interactions. Plant J. *114*, 1209–1226.
44. Bhattacharjee, S., Halane, M.K., Kim, S.H., and Gassmann, W. (2011). Pathogen effectors target Arabidopsis EDS1 and alter its interactions with immune regulators. Science *334*, 1405–1408.
45. Heidrich, K., Wirthmueller, L., Tasset, C., Pouzet, C., Deslandes, L., and Parker, J.E. (2011). Arabidopsis EDS1 connects pathogen effector recognition to cell

compartment-specific immune responses. Science *334*, 1401–1404.

46. Huh, S.U., Cevik, V., Ding, P., Duxbury, Z., Ma, Y., Tomlinson, L., Sarris, P.F., and Jones, J.D.G. (2017). Protein-protein interactions in the RPS4/RRS1 immune receptor complex. PLoS Pathog. *13*, e1006376.
47. Kim, T.H., Kunz, H.H., Bhattacharjee, S., Hauser, F., Park, J., Engineer, C., Liu, A., Ha, T., Parker, J.E., Gassmann, W., and Schroeder, J.I. (2012). Natural variation in small molecule-induced TIR-NB-LRR signaling induces root growth arrest via EDS1- and PAD4-complexed R protein VICTR in Arabidopsis. Plant Cell *24*, 5177–5192.
48. Sun, X., Lapin, D., Feehan, J.M., Stolze, S.C., Kramer, K., Dongus, J.A., Rzemieniewski, J., Blanvillain-Baufumé, S., Harzen, A., Bautor, J., et al. (2021). Pathogen effector recognition-dependent association of NRG1 with EDS1 and SAG101 in TNL receptor immunity. Nat. Commun. *12*, 3335.
49. Wang, H., Song, S., Gao, S., Yu, Q., Zhang, H., Cui, X., Fan, J., Xin, X., Liu, Y., Staskawicz, B., and Qi, T. (2023). The NLR immune receptor ADR1 and lipase-like proteins EDS1 and PAD4 mediate stomatal immunity in Nicotiana benthamiana and Arabidopsis. Plant Cell *1*, koad270.
50. Wu, Z., Tian, L., Liu, X., Huang, W., Zhang, Y., and Li, X. (2022). The N-terminally truncated helper NLR NRG1C antagonizes immunity mediated by its full-length neighbors NRG1A and NRG1B. Plant Cell *34*, 1621–1640.
51. Wang, Z., Liu, X., Yu, J., Yin, S., Cai, W., Kim, N.H., El Kasmi, F., Dangl, J.L., and Wan, L. (2023). Plasma membrane association and resistosome formation of plant helper immune receptors. Proc. Natl. Acad. Sci. USA *120*, e2222036120.
52. Bernoux, M., Timmers, T., Jauneau, A., Brière, C., de Wit, P.J.G.M., Marco, Y., and Deslandes, L. (2008). RD19, an Arabidopsis cysteine protease required for RRS1-R-mediated resistance, is relocalized to the nucleus by the Ralstonia solanacearum PopP2 effector. Plant Cell *20*, 2252–2264.
53. Cesari, S., Moore, J., Chen, C., Webb, D., Periyannan, S., Mago, R., Bernoux, M., Lagudah, E.S., and Dodds, P.N. (2016). Cytosolic activation of cell death and stem rust resistance by cereal MLA-family CC-NLR proteins. Proc. Natl. Acad. Sci. USA *113*, 10204–10209.
54. Saur, I.M., Bauer, S., Kracher, B., Lu, X., Franzeskakis, L., Müller, M.C., Sabelleck, B., Kümmel, F., Panstruga, R., Maekawa, T., and Schulze-Lefert, P. (2019). Multiple pairs of allelic MLA immune receptor-powdery mildew AVRA effectors argue for a direct recognition mechanism. Elife *8*, e44471.
55. Alberti, S., Gitler, A.D., and Lindquist, S. (2007). A suite of Gateway (R) cloning vectors for high-throughput genetic analysis in Saccharomyces cerevisiae. Yeast *24*, 913–919.
56. Kushnirov, V.V. (2000). Rapid and reliable protein extraction from yeast. Yeast *16*, 857–860.
57. Cesari, S., Thilliez, G., Ribot, C., Chalvon, V., Michel, C., Jauneau, A., Rivas, S., Alaux, L., Kanzaki, H., Okuyama, Y., et al. (2013). The Rice Resistance Protein Pair RGA4/RGA5 Recognizes the Magnaporthe oryzae Effectors AVR-Pia and AVR1-CO39 by Direct Binding. Plant Cell *25*, 1463–1481.

## STAR★METHODS

### KEY RESOURCES TABLE

| REAGENT or RESOURCE | SOURCE | IDENTIFIER |
|---|---|---|
| **Antibodies** | | |
| Rat anti-HA-Peroxidase | Roche | Roche Cat# 12013819001; RRID: AB_390917 |
| Mouse anti-GFP | Roche | Sigma-Aldrich Cat# 11814460001; RRID: AB_390913 |
| Mouse anti-*c*-Myc | Roche | Roche Cat# 11667149001; RRID: AB_390912 |
| Goat anti-Mouse HRP Conjugate | Bio-Rad | Bio-Rad Cat# 170-5047; RRID: AB_11125753 |
| Polyclonal rabbit anti-luciferase | Sigma-Aldrich | Sigma-Aldrich Cat# L0159; RRID: AB_260379 |
| Rabbit anti-GAL4 DNA-BD antibody | Sigma-Aldrich | Sigma-Aldrich Cat# G3042; RRID: AB_439688 |
| Rabbit anti-VP16 antibody | Sigma-Aldrich | Sigma-Aldrich Cat# V4388; RRID: AB_261865 |
| Goat anti-rabbit HRP | Invitrogen | Thermo Fisher Scientific Cat# 65-6120; RRID: AB_2533967 |
| **Bacterial and virus strains** | | |
| *Agrobacterium tumefaciens* strain GV3101_pMP90 | Kept in lab stock | N/A |
| *Agrobacterium tumefaciens* strain GV3103 | Kept in lab stock | N/A |
| *Escherichia coli* DH5α | Kept in lab stock | N/A |
| **Chemicals, peptides, and recombinant proteins** | | |
| Phusion™ High-Fidelity DNA Polymerase | ThermoFisher | # F-530XL |
| BP clonase | Invitrogen | #11789020 |
| LR clonase | Invitrogen | #11791020 |
| Acetosyringone | Sigma-Aldrich | #D134406 |
| Premium Western blotting membranes, nitrocellulose | Amersham | #GE10600009 |
| Ponceau S | Sigma-Aldrich | #P3504 |
| Kanamycin | Sigma-Aldrich | #K1377 |
| Gentamycin | Sigma-Aldrich | #G1264 |
| Carbenicillin | Sigma-Aldrich | #C1389 |
| Chloramphenicol | Sigma-Aldrich | #C0378 |
| Rifampicin | Sigma-Aldrich | #R3501 |
| **Critical commercial assays** | | |
| PureLink™ PCR Purification Kit | Thermo Scientific | #K310001 |
| QIAprep Spin Miniprep Kit | QIAGEN | #27106 |
| Cell Culture Lysis 5X Reagent | Promega | #E1531 |
| Luciferase substrate | Promega | #E1501 |
| GFP-Trap Magnetic Agarose beads | Chromotek | # gtma-20 |
| **Deposited data** | | |
| original immunoblot images were deposited on Mendeley | https://data.mendeley.com/preview/rptr929dd8?a = 3cfbe02f-4002-4ced-bdc1-96abdd2ff130 | DOI: https://doi.org/10.17632/rptr929dd8.1 |
| **Experimental models: Organisms/strains** | | |
| *Nicotiana benthamiana* | Kept in lab | N/A |
| *N. benthamiana* mutant line *eds1* | provided by B. Staskawicz | Ref. 27 |
| *N. benthamiana* mutant line *eds1pad4* | provided by J. Stuttmann | Ref. 34 |
| *N. benthamiana* mutant line *pad4sag101a/b* | provided by J. Stuttmann | Ref. 34 |
| *N. benthamiana* mutant line *nrg1* | provided by J. Stuttmann | Ref. 40 |

(*Continued on next page*)

*Continued*

| REAGENT or RESOURCE | SOURCE | IDENTIFIER |
|---|---|---|
| Oligonucleotides | | |
| Primers used for DNA amplification, molecular cloning and site-directed mutagenesis are shown in Table S1 | This study | Table S1 |
| Recombinant DNA | | |
| pGADT7-GWY | lab stock | N/A |
| pGBKT7-GWY | lab stock | N/A |
| pAG416GPD-GWY | Addgene | #14244 |
| pAM-PAT-GWY-YFPv | lab stock | N/A |
| pAM-PAT-GWY-3xHA | lab stock | N/A |
| pAM-PAT-GWY-3Myc | lab stock | N/A |
| pBIN19-YFP-GTW | lab stock | N/A |
| pBIN19-HA-GTW | lab stock | N/A |
| pBIN19-GWY-CFP | lab stock | N/A |
| pDONR207 | lab stock | N/A |
| pDEST-GWY-nLUC | University of Munster | Ref. 42 |
| pDEST-GWY-cLUC | University of Munster | Ref. 42 |
| pAM-PAT-VP16-GWY | lab stock | N/A |
| pAM-PAT-GWY-GALBD | lab stock | N/A |
| Recombinant plasmids used in this study are listed in Tables S2 and S3 | This study | Tables S2 and S3 |
| Software and algorithms | | |
| GraphPad Prism 10.0.3 | GraphPad | https://www.graphpad.com |
| Pymol | Schrödinger Inc. | https://pymol.org |

## RESOURCE AVAILABILITY

### Lead contact

Further information and requests for resources should be directed to and will be fulfilled by the lead contact, Dr. Peter Dodds (peter.dodds@csiro.au).

### Materials availability

- Plasmids generated in this study are available from the lead contact with a completed Materials Transfer Agreement.
- This study did not generate new unique reagents.

### Data and code availability

- This study did not generate standardised datasets. Original western blot images were deposited on Mendeley with the following DOI: https://doi.org/10.17632/rptr929dd8.1; https://data.mendeley.com/preview/rptr929dd8?a=3cfbe02f-4002-4ced-bdc1-96abdd2ff130.
- This study did not generate original code.
- Any additional information required to reanalyze the data reported in this paper is available from the lead contact upon request.

## EXPERIMENTAL MODEL AND STUDY PARTICIPANT DETAILS

### Plant growth

*Nicotiana benthamiana* was used in this study. *N. benthamiana* plants carrying CRSIPR/Cas9-generated mutants were described previously (*eds1*[27]; *eds1/pad4* and *pad4/sag101a/sag101b*,[34] and *nrg1*[40]). Seeds were sown in Debco mix with 2 g/L Osmocote and after 10 days individual seedlings were transplanted into 12 cm diameter pots with Scotts Premium Mix soil with 4 g/L Osmocote. Plants were grown under controlled environmental conditions at 23°C with a 16-h light period (light intensity 10 klux). Plants were used for infiltration 3–4 weeks after transplanting.

### Bacterial growth

For leaf infiltration, constructs were transformed into *Agrobacterium tumefaciens* strain GV3103_pMP90 (pAM-PAT constructs) or GV3101_pMP90 (pBIN19 and pDEST-GWY-nLUC/cLUC constructs) by electroporation. Cultures were grown at 28°C with shaking overnight in Luria-Bertani liquid medium containing 25 μg/mL of rifampicin, 15 μg/mL gentamicin and either 50 μg/mL of kanamycin (pBIN19 and pDEST vectors) or 25 μg/mL of carbenicillin (pAM-PAT vectors). Cells were harvested by centrifugation, resuspended in infiltration buffer (10 mM MES pH 5.6, 10 mM MgCl2 and 150 μM acetosyringone) and incubated at room temperature for 2 h.

## METHOD DETAILS

### Generation of constructs

Details of primers and constructs used here are shown in Tables S1–S3. All new constructs were generated by Gateway cloning (GWY; Invitrogen), with Phusion High-Fidelity DNA Polymerase (Thermo Fisher) used for PCR amplification of fragments flanked by attB sites for recombination into pDONR207 (BP reaction) and then into destination vectors (LR reaction). The binary vector pAM-PAT-35s-GWY-YFPv (or with 3xHA or 3xMyc tags)[52] was used for all *in planta* cell death and CoIP experiments, except for *Nb*NRG1 and *Nb*ADR1 for which the pBIN19-GWY-CFP (or 3xHA tag) vector[53] was also used. The TIR-NLRC4 fusion constructs were previously described.[16] For Split-Luciferase assays, genes were cloned into the binary vectors pDEST-GWY-nLUC and pDEST-GWY-cLUC.[42,54] For yeast two-hybrid and three-hybrid experiments, cDNAs were cloned into Gateway-compatible yeast two-hybrid vectors based on pGADT7 and pGBKT7 (Clontech) or into the pAG416GPD-ccdB-HA vector[55] (pAG416GPD-ccdB-HA was a gift from Susan Lindquist (Addgene plasmid # 14244; http://n2t.net/addgene:14244; RRID: Addgene_14244)). Mutations were generated by DpnI-mediated site-directed mutagenesis (Stratagene). For plant two-hybrid assays, genes were cloned into the binary vectors pAM-PAT-GWY-BD and pAM-PAT-VP16-GWY.[43]

### Transient expression in *N. benthamiana*

Plants were grown at 23°C with a 16-h light period. For leaf infiltration, constructs were transformed into *Agrobacterium tumefaciens* strain GV3103 (pAM-PAT constructs) or GV3101_pMP90 (pBIN19 and pDEST-GWY-nLUC/cLUC constructs) by electroporation. Cultures were grown at 28°C with shaking overnight in Luria-Bertani liquid medium containing 25 μg/mL of rifampicin, 15 μg/mL gentamicin and either 50 μg/mL of kanamycin (pBIN19 and pDEST vectors) or 25 μg/mL of carbenicillin (pAM-PAT vectors). Cells were harvested by centrifugation, resuspended in infiltration buffer (10 mM MES pH 5.6, 10 mM MgCl2 and 150 μM acetosyringone) and incubated at room temperature for 2 h. The final bacterial concentration for cell death complementation and Co-IP assays was OD600 = 0.5. Three to four individual plants were infiltrated for each combination of constructs and experiments were repeated at least three times. Plants were infiltrated 3–4 weeks after transplanting in the third and fourth leaves counting from the youngest apical leaf, which give the most robust cell death responses under our conditions. However, in *nrg1* mutant plants the 3$^{rd}$/4$^{th}$ leaves consistently showed a non-specific cell death response to *Agrobacterium* infiltration, so we used the 5$^{th}$ and 6$^{th}$ leaves which did not show non-specific cell death but gave a generally weaker response than the 3$^{rd}$/4$^{th}$ leaves of wild-type plants. Leaves were scanned 3–5 days after infiltration to record cell death responses.

### Yeast two-hybrid and yeast three-hybrid assays

Transformation of *Saccharomyces cerevisiae* strain HF7c was performed as described in the Yeast Protocols Handbook (Clontech), with transformants selected on synthetic dropout (SD) medium lacking tryptophan and leucine (-WL) to select for pGADT7 and pGBKT7 plasmids, or additionally lacking Uracil (-WLU) to select for pAG416GPD vectors. To assess protein interactions, three independent colonies were grown on medium lacking leucine, tryptophan, and histidine (-HWL two-hybrid) or also lacking uracil (-HWLU, three-hybrid) at 30°C for 3–4 days.

### Split-luciferase and plant two-hybrid assays

The split-luciferase (Split-LUC) complementation assay was performed as previously described.[54] Three disks (0.38 cm diameter) from three independent leaves were harvested into 1.5 mL tube two days after infiltration at 4-week-old *N. benthamiana* plants. Samples were ground to fine powder using pestles on dry ice and then 100 μL 2x cell culture lysis buffer was added (Promega, E1531; with 150 mM Tris-Hcl pH7.5). 50 μL of leaf extract was mixed with 50 μL luciferase substrate (Promega, E1501) in a white-bottomed 96-well plate, and the light emission was measured using a microplate luminometer (Fluostar Omega) at 1 s/well. The final Agrobacterium concentration of each construct was OD600 = 1.5, except for the pDEST-LLD-*Nb*EDS1-cLUC, pDEST-*Nb*SAG101b-cLUC and pDEST-*Nb*PAD4-cLUC, which was OD600 = 0.15 as these constructs showed higher protein expression than other pDEST constructs. For plant two-hybrid assays, four-week-old *N. benthamiana* plants were used for the infiltration of Agrobacteria containing UAS-Ruby and TIR/EDS1 constructs. Whole leaves were harvested 3–5 days after infiltration and scanned and then cleared using ethanol. Three disks from three independent decolourised leaves were collected in a 1.5 mL tube with 0.5 mL water to extract betalain. The absorbance of betalain was measured at 538 nm. The Agrobacterium concentration was OD600 = 0.2 for the pAM-TIR-BD constructs, and OD600 = 0.8 for the pAM-VP16-*Nb*EDS1 constructs.

### Protein extraction, immunoblot, and coimmunoprecipitation

For immunoblot analysis, proteins were extracted from plant tissues directly into loading buffer (0.125 M Tris-HCl, pH 7.5, 4% SDS, 20% Glycerol, 0.2 M DTT, 0.02% Bromophenol Blue) while yeast protein extraction was performed following a post-alkaline method.[56] For co-immunoprecipitation experiments agrobacterium cultures were infiltrated at OD600 = 0.5 and proteins were extracted as previously described.[57]

For immunodetection, proteins were separated by SDS-PAGE and transferred to nitrocellulose membranes which were blocked in 5% skimmed milk. Membranes were incubated with Anti-HA-Peroxidase, High Affinity (Roche, ref. 12013819001) or mouse anti-GFP (Roche, ref. 11814460001) and anti-Myc antibodies (Roche, ref. 11667149001) followed by goat anti-mouse antibodies conjugated with horseradish peroxidase (Biorad, ref. 170–5047), or polyclonal rabbit anti-luciferase (Sigma-Aldrich, REF L0159), anti-GAL4BD (Sigma-Aldrich, REF G3042) and anti-VP16 (Sigma-Aldrich, REF V4388) antibodies followed by anti-rabbit horseradish peroxidase (Sigma) to detect -HA, YFP, Myc, nLUC, cLUC, GAL4BD and VP16 tagged proteins respectively. Signals were detected using the SuperSignal West Femto chemiluminescence kit (Pierce). Ponceau S was used to stain membranes to confirm equal protein loading.

## QUANTIFICATION AND STATISTICAL ANALYSIS

Data were analyzed and presented as box and whisker plots using the GraphPad Prism 10.0.3, the horizontal line in the graphs indicate the median. Statistical significance of differences for Figures 3A and 3B was performed with one-way-ANOVA by LSD test, $p < 0.05$. The letters on the top of each column indicate statistically differences between different tests. The significance of differences for Figures 3C–3E and S11D was analyzed with student's unpaired, two-tailed t-test was performed to compare differences between groups in each experiment (***$p < 0.001$; **$p < 0.01$; *$p < 0.05$).